# Two Distinct Functions of the Carboxyl-terminal Tail Domain of NF-M upon Neurofilament Assembly: Cross-bridge Formation and Longitudinal Elongation of Filaments

Terunaga Nakagawa, Jianguo Chen, Zhizeng Zhang, Yoshimitsu Kanai, and Nobutaka Hirokawa

Department of Anatomy and Cell Biology, University of Tokyo, Faculty of Medicine, Bunkyo-ku, Tokyo 113, Japan

*Abstract.* Neurofilaments are the major cytoskeletal elements in the axon that take highly ordered structures composed of parallel arrays of 10-nm filaments linked to each other with frequent cross-bridges, and they are believed to maintain a highly polarized neuronal cell shape. Here we report the function of rat NF-M in this characteristic neurofilament assembly. Transfection experiments were done in an insect Sf9 cell line lacking endogenous intermediate filaments. NF-L and NF-M coassemble to form bundles of 10-nm filaments packed in a parallel manner with frequent cross-bridges resembling the neurofilament domains in the axon when expressed together in Sf9 cells. Considering the fact that the expression of either NF-L or NF-M alone in these cells results in neither formation of any ordered network of 10-nm filaments nor cross-bridge structures, NF-M plays a crucial role in this parallel filament assembly. In the case of NF-H the

carboxyl-tail domain has been shown to constitute the cross-bridge structures. The similarity in molecular architecture between NF-M and NF-H suggests that the carboxyl-terminal tail domain of NF-M also constitutes cross-bridges. To examine this and to further investigate the function of the carboxyl-terminal tail domain of NF-M, we made various deletion mutants that lacked part of their tail domains, and we expressed these with NF-L. From this deletion mutant analysis, we conclude that the carboxyl-terminal tail domain of NF-M has two distinct functions. First, it is the structural component of cross-bridges, and these cross-bridges serve to control the spacing between core filaments. Second, the portion of the carboxyl-terminal tail domain of NF-M that is directly involved in cross-bridge formation affects the core filament assembly by helping them to elongate longitudinally so that they become straight.

A MONG the three major cytoskeletal structures (actin filaments, microtubules, and intermediate filaments), intermediate filaments are different from the other two in several ways. First different cell types within an organism have their distinct intermediate filament proteins that polymerize into 10-nm diameter filaments, which appear similar in structure when viewed by electron microscopy. Second, the monomers of each intermediate filament protein have a common molecular motif that consists of a globular head domain, alpha-helical rod domain, and carboxyl-terminal tail domain, whereas actin and tubulin are globular proteins. Finally, what is most important is that much less is known about their dynamics, functions, and structure compared to actin filaments and microtubules.

In adult neurons, neurofilaments are the major cytoskeletal elements that are composed of three different subunits

called NF-L, NF-M, and NF-H (Willard and Simon, 1981; Hirokawa et al., 1984), and they are classified as the type IV intermediate filaments. They are believed to support the highly polarized morphology of axons, and several lines of evidence have shown that their abundance in an axon correlates with its caliber (Friede and Samorajski 1970; Lasek et al., 1983; Hoffman et al., 1985). Supporting this, fewer numbers of neurofilaments are found in the nodes of Ranvier, where the caliber is reduced within the same axon. The transport of neurofilaments controls axonal caliber (Hoffman et al., 1984, 1987). Transgenic model mice of amyotrophic lateral sclerosis give rise to the idea that aggregation of neurofilaments in the cell body causes blockage in axonal transport, resulting in thin axons with few neurofilaments (Zu et al., 1993; Cote et al., 1993; Lee and Cleveland, 1994). Other transgenic mice overexpressing NF-H fused to lacZ accumulate neurofilaments in cell bodies, and they have smaller axonal calibers compared to wild-type mice (Eyer and Peterson, 1994). The relationship between axon caliber and neurofilament abundancy is further explained at the ultrastructural level by recent studies involving neurofilament triplet proteins and microtubule-associated proteins.

Address correspondence to Nobutaka Hirokawa, Department of Anatomy and Cell Biology, University of Tokyo, Faculty of Medicine, 7-3-1 Hongo, Bunkyo-ku, Tokyo 113, Japan. Tel.: (81) 3-3812-2111, ext. 3326. Fax: (81) 3-5689-4856.

Neurofilaments assume characteristic structures in axons distinct from other intermediate filaments such as desmins, vimentins, and glial fibrillary acidic protein (GFAP). First, respective neurofilaments run in parallel to each other to form bundles. Second, between each pair of filaments, frequent cross-bridges are observed (Hirokawa, 1982). The 10-nm diameter filaments are called "core filaments" to distinguish them from cross-bridge structures. These cross-bridges are thought to retain the spacing between respective filaments, as is the case with microtubules in which cross-bridges formed by tau and MAP2 determine the intermicrotubule spacings (Chen et al., 1992). We hypothesize that cross-bridges in neurofilaments are the ultimate structural elements that are responsible for axon caliber maintenance. Thus, the studies of these cross-bridges are of great interest. Immunocytochemistry has shown that an anti–NF-H antibody that recognizes the carboxyl-terminal tail domain binds to cross-bridges of neurofilaments in adult axons, whereas anti–NF-M antibody mainly decorates the core filaments. (Hirokawa et al., 1984) This carboxyl terminus tail domain of NF-H is thought to be a component of cross-bridges between neurofilaments. It also plays important roles in the interaction between neurofilaments and microtubules (Hisanaga and Hirokawa, 1990a; Miyasaka et al., 1993). In contrast, however, the function of NF-M is least known.

In vitro reconstitution studies observed by low angle rotary shadowing tell us that NF-L assembles to form the core filaments (Hisanaga and Hirokawa, 1988, 1990b). Thin projections appear from these core filaments only when NF-M or NF-H is added, which probably corresponds to cross-bridges in vivo (Hisanaga and Hirokawa, 1988). Even when copolymerized with NF-M or NF-H, neurofilaments reconstituted in vitro do not form bundles such as those in vivo. On the other hand, in vivo reconstitution studies in fibroblasts lacking endogenous intermediate filaments investigated by immunofluorescence reveal that neurofilaments are obligate heteropolymers (Lee et al., 1993; Ching and Liem, 1993). In detail, no apparent filamentous staining was observed in fibroblasts transfected only with NF-L, and they require the addition of NF-M or NF-H for filaments to be detected by the immunofluorescence staining.

Although NF-L forms 10-nm filaments in vitro (Hisanaga and Hirokawa, 1988, 1990b), no filamentous immunofluorescence staining was observed in fibroblasts transfected with NF-L cDNA (Lee et al., 1993; Ching and Liem, 1993) This could be explained as follows. In fibroblasts transfected with NF-L, the filaments are either not formed, or they are formed too short and compact to be detected by immunofluorescence resolution. If the former is the case, NF-L may be flexibly changing its assembly properties in an environmentally dependent manner. Thus, there is a possibility that the assembly properties of NF-L may differ between in vitro and in vivo reconstitution and no doubt its coassembly properties with NF-M and NF-H. Needless to say, in vivo reconstitution studies by transfection should be more reliable. If neurofilament assembly properties change when they are moved outside of the cell, do the phenomena observed in in vitro reconstitution really reflect what takes place in vivo? Do the loose projections hanging out from the core filaments that were observed by rotary shadowing really represent the cross-bridge structures seen in axons, and are they the carboxyl-terminal tail domain? Do NF-L with NF-M or NF-H form highly ordered neurofilament arrays observed in

axons in transfected cells? In other words, since there is no information about the fine structures formed by the transfected neurofilament proteins in in vivo reconstitution studies, it is not known whether the immunofluorescence staining in fibroblast transfection is formed by the highly ordered ultrastructure characteristic of neurofilaments in axons. In this context, it is definitely necessary to observe the in vivo reconstitution of neurofilaments, especially for NF-L and NF-M, by high resolution such as quick-freeze, deep-etch electron microscopy. Thus, we investigated the ultrastructures of the transfected NF-L and NF-M.

Transfections were done by infecting nonneuronal insect Sf9 cells with recombinant baculovirus vectors encoding NF-L and NF-M. Sf9 cells are derived from IPLB-Sf21 cells, which are known immunocytochemically not to possess any types of intermediate filaments that are conserved among other species (Volkman and Zaal, 1990). Generally, crustaceans have no intermediate filaments (Hirokawa, 1986; Hirokawa and Yorifuji, 1986; Viancour et al., 1987), so it is not unreasonable to suppose that certain cells of some insects in the same arthropods do not have intermediate filaments. Indeed, we found no intermediate filaments in the cytoplasm of Sf9 cells. So we identified this Sf9 baculovirus system as an ideal system for studying the assembly of intermediate filaments, especially for neurofilaments, because in past studies the pure assembly environment in transfection experiments was disturbed by their property to copolymerize with endogenous vimentins (Chin and Liem, 1989; Monterio and Cleveland, 1989; Wong and Cleveland, 1990; Chin et al., 1991). Another advantage of this system is that electron microscopy analysis is facilitated, as high level expression and transfection efficiency can be expected.

Furthermore, to prove that the carboxyl-terminal tail domain of NF-M is actually involved in cross-bridge formation, we constructed various deletion mutants of NF-M lacking part of is its tail and transfected them into Sf9 cells together with NF-L. By this deletion mutant analysis, we also found an unexpected function of the tail domain as well.

## Materials and Methods

### Insect Cell Culture

Sf9 cells were grown in TNM-FN medium containing 10% fetal calf serum. Cells were incubated at 27°C in plastic dishes or bottles, and they were split approximately every 2 d so that the cells did not float into the media by overgrowing. Details are available in the literature (O'Reilly et al., 1992).

### Construction of Baculovirus Transfer Vectors

All recombinant DNA protocols are based on those in the literature of Sambrook et al. (1989).

Because both genes were already cloned by others (Napolitano et al., 1987; Levy et al., 1987), the cDNAs of NF-L and NF-M genes were obtained by PCR and lamda gt-10 rat brain cDNA library screening, respectively. Partial fragments of each gene were kindly provided by Dr. N. Cowan (New York University, Medical Center, New York), and they were used as a probe for screening. All fragments that were amplified by PCR were sequenced by autosequencer (model 375; Applied Biosystems Inc., Foster City, CA). NF-L was subcloned between BamHI and EcoRI sites of pBS SK (+). The start codon was in close proximity to BamHI site. This subcloning vector including the whole NF-L open reading frame was named pBL. NF-M was subcloned into the EcoRI site of pBS SK(+). The start codon of NF-M was in close proximity to the EcoRV site of pBS SK(+). This subcloning vector, including the whole open reading frame of NF-M, was named pBM. Three transfer vector constructs were built from the cloned genes: pNFL, pNFM, and pNFLM.

To construct pNFL, a BamHI-EcoRI fragment containing the whole open reading frame of NF-L, was inserted between BamHI and EcoRI sites of pVL1393 so that the NF-L gene would be under the control of the polyhedrin promoter. To construct pNFM, BglII linker was inserted into the EcoRV site of pBM. This vector was then digested with BglII and XbaI to get a 2.6-kb fragment, and it was inserted between the BamHI and XbaI sites of pVL1393. To construct pNFLM, the same BamHI-EcoRI fragment of NF-L was first inserted between the BglII and EcoRI sites of pAcUW51. 2.6-kb BglII-BamHI NF-M fragment was then cut out from pBM and inserted in correct direction into the BamHI site of pAcUW51 already containing NF-L. In pNFLM, NF-L and NF-M genes are under control of the p10 and polyhedrin promoters, respectively.

## Production of Recombinant Baculoviruses

Recombinant baculoviruses were produced by cotransfecting linealized baculovirus DNA with transfer vectors into Sf9 cells. BAKPAK6 (Clontech Laboratories, Palo Alto, CA) -linealized DNA and lipofectin (GIBCO BRL, Gaithersburg, MD) were used as reagents. The profiles of the recombinant baculoviruses used in this study are listed in Table I.

## Construction of Deletion Mutant Transfer Vector

Six different deletion mutants were constructed as listed in Fig. 8. There is a unique SacI site in the rod domain of the NF-M cDNA clone close to the beginning of the tail domain. Sequences between this SacI site and stop codon were excluded from the vector, and they were exchanged with newly generated fragments amplified by PCR. Myc epitopes were attached to the carboxyl-terminal of each deletion mutant by including this sequence into the PCR primers. Each amplified fragment was sequenced by an Applied Biosystems autosequencer. All deletion NF-M clones were subcloned into the BglII site downstream the p10 promoter of pAcUW51, which already contains NF-L under control of the polyhedrin promoter.

## Western Blots

Expression of NF-L and NF-M by each recombinant baculovirus was confirmed by Western blot analysis. Sf9 cells were infected with baculoviruses encoding NF-L alone, NF-M alone, or NF-L and NF-M together. Total homogenates of Sf9 cells infected with each baculovirus were resolved on 7.5% SDS-polyacrylamide gel, and they were probed with anti-NF-L monoclonal antibody (RPN1105; Amersham Corp. Arlington Heights, IL) and with anti-NF-M monoclonal antibody (NN18). Noninfected native Sf9 cell total homogenates were also loaded onto a different lane, and they were probed with both antibodies as controls. All cell lysates were prepared by adding SDS loading buffer directly into Sf9 cells that had been briefly washed with PBS. Peroxydase-conjugated anti-mouse IgG antibody (Cappel Laboratories, Cochranville, PA) was used as a second antibody. Chromogenic reaction was done by 4-chloro-1-naphthol.

Expression of neurofilament proteins encoded by the recombinant baculovirus encoding NF-L and deletion mutants of NF-M were also checked by Western blotting in the same manner. Monoclonal antibody against myc epitope was used to detect deletion mutants. Monoclonal antibody SMI31 (Sternberger and Sternberger, 1983; Lee et al., 1988; Harris et al., 1991) was used to detect NF-M that is phosphorylated in the carboxyl-terminal tail domain. IFA monoclonal antibody (Pruss et al., 1981) was kindly provided as overgrown culture supernatant by Dr. K. Weber (Max-Planc-Institute for Biophysical Chemistry, Groettingen, FRG), and it was used to detect DelmImyc(−). IFA was used as described (Pruss et al., 1981), except that peroxydase-conjugated anti-mouse IgG antibody (Cappel) was used as a second antibody, and that chromogenic reaction was done by 4-chloro-1-naphthol.

## Densitometry Analysis

Cytoskeletal fractions of Sf9 cells infected with each of the viruses were extracted by treating the cells with 1% Triton X-100 1 mM PMSF, 10 ng/ml leupeptin in PEM buffer (100 mM Pipes, 1 mM EGTA, and 1 mM MgCl$_2$, pH 6.8) for 10 min, and collecting the pellet by centrifuge. This pellet was resuspended into SDS-PAGE loading buffer and resolved by SDS-PAGE. Gels were stained with Coomassie blue and dried for densitometry analysis. The Quantity One System program (Pharmacia Fine Chemicals, Piscataway, NJ) in a PDI image analyzer was used for measurement.

## First-strand cDNA Synthesis Assay

Total RNA of mouse brain and Sf9 cells were extracted and purified by

cesium trifluoroacetate method, and polyadenilated RNA was further collected by oligo(dT) cellulose chromatography, as described in the literature of Okayama et al. (1987). 500 ng of poly(A)$^+$ RNA from brain and Sf9 cells were reverse transcribed by incorporating $^{32}$P-dCTP using a 27-bp primer (5'-ATG TT(T/C) TT(T/C) GAI GAI CT(T/C) CCI CT(T/C) CT-(T/C)-3'), which recognizes both the IFA epitope of vertebrates (YRKLLE-GEE) and the IFA epitope-like amino acid sequence found in invertebrates (YKKLLEGEE). This primer anneals with the nucleotide sequence in mRNA, which corresponds to amino acid sequences (YRKLLEGEE) and (YKKLLEGEE). 500 ng of poly(A)$^+$ RNA from mouse brain and Sf9 cells were taken from 500 ng/$\mu$l poly(A)$^+$ RNA stock solution and diluted in 3.5 $\mu$l of 5 mM Tris HCl, pH 7.5. After heating at 65°C for 5 min, the samples were put into a 37°C incubator, and the following mixture was added: 10× reverse transcribed (RT)[1] buffer (500 mM Tris HCl pH 8.5, at 20°C, 80 mM MgCl$_2$, 300 mM KCl, and 3 mM dithiothreitol), 1.5 $\mu$l; 20 mM dNTP, 1.5 $\mu$l; reverse transcriptase (23 U), 1 $\mu$l; [$^{32}$P]dCTP (100 $\mu$Ci), 0.5 $\mu$l; H$_2$O, 5 $\mu$l. Then the samples were incubated at 37°C for 30 min. After incubation, the samples were extracted with phenol/chloroform and precipitated with ethanol twice using ammonium acetate as salt to remove the unincorporated dNTPs. The precipitated DNA/RNA hybrid was resuspended in 10 $\mu$l of sample buffer (30 mM NaOH, 10% glycerol, 2 mM EDTA, pH 8.0, and 0.5% bromocresol blue), and it was applied to 1% agarose alkaline denature gel containing 30 mM NaOH and 2 mM EDTA, pH 8.0. 30 mM NaOH and 10 mM EDTA, pH 8.0, was used as running buffer. After electrophoresis, the gel was washed in 250 ml of 10 mM EDTA, pH 8.0, for 1 h twice and once in 2× SSC for 30 min at room temperature to remove sodium hydroxide. Then the samples were transferred onto a nylon membrane with 20× SSC. The membrane was dried and exposed to an image analyzing plate (BAS 2000; Fuji (Fuji Film; Tokyo, Japan) for 2 h to detect signals.

## Immunofluorescence Microscopy

Sf9 cells were grown on polylysine-coated coverslips in 35-mm plastic dishes. Cells were fixed at 38 h after infection with each of the viruses. After fixation with 2% paraformaldehyde and 0.1% glutaraldehyde (PBS, pH 6.2) for 5 min, the cells were permeabilized with methanol at −20°C for 5 min, and quenched with 1 mg/ml NaBH$_4$ in PBS. Blocking was done at room temperature in 5% BSA in PBS for at least 15 min. The following were used: monoclonal antibody against NF-L (RPN 1105; Amersham), NF-M (NN18), polyclonal antibody against NF-L (CMN AB 1983), and for detecting deletion mutants of NF-M, anti-myc monoclonal antibody (Boehringer Mannheim Biochemicals, Indianapolis, IN). The samples were incubated at 37°C for 1 h with primary antibodies diluted in blocking solution. FITC-conjugated anti-mouse IgG and rhodamine-conjugated anti-rabbit IgG were used as secondary antibodies (at 37°C for 1 h). Samples were mounted on cover glass with mounting media (50% glycerol, PBS). Immunofluorescence micrographs were taken by Axiophot (Carl Zeiss, Inc., Thornwood, NY) with TMAX400 film (Eastman Kodak Co., Rochester, NY).

Sf9 cells infected with the L+DelMlmyc(−) virus were double stained with the anti-NF-L polyclonal antibody described above and IFA monoclonal antibody. Fixatives, working dilution, and blocking solution for the primary antibodies were followed as described elsewhere (Pruss et al., 1981). The rest of the procedures were conducted as described above, except that the samples were viewed with a confocal microscope. 18 slices were taken every 0.98 $\mu$m to observe a single cell. Kodak Dyna 100 film was used.

## Ultrathin Section Electron Microscopy

*Nonpermeabilizing Protocol.* Sf9 cells were washed briefly with PBS in a suspension, and they were collected by mild centrifugation. Cell pellets were resuspended in a fixative (2.5% glutaraldehyde and 2% paraformaldehyde in 0.1 M cacodylate buffer, pH 7.4), and they were fixed at room temperature for 30 min. Cells were again centrifuged for collecting, and the supernatant was discarded. After brief washing with 0.1 M cacodylate buffer, 0.1 M cacodylate buffer, pH 7.4, with 1% OsO$_4$ was gently added to these pellets, and they were incubated on ice for 1.5 h. The tubes were inverted several times during incubation. After osmification, the cells were washed with distilled water, and they were block stained in 1% uranyl acetate for 1 h. Cell pellets were dehydrated with ethanol and propylene oxide, and were then incubated in Epon/propylene oxide 1:1 mixture for 1 d. Finally, the cell pellets were embedded in Epon in beam capsules. Before solidifying at 65°C, samples were centrifuged so that the pellets dropped to the bottom of the tubes. Embedded samples were trimmed and sectioned

---

1. *Abbreviation used in this paper*: RT, reverse-transcribed.

on an ultramicrotome. Ultrathin sections were double stained with uranyl acetate and lead citrate, and they were viewed with an electron microscope (1200EX or 2000EX; JEOL U.S.A. Inc., Peabody, MA).

*Permeabilizing Protocol.* Sf9 cells were briefly washed with PBS in suspension and collected by centrifugation. For mild permeabilizing, this cell pellet was resuspended in a detergent buffer (0.05% saponin and 2 mM GTP in PBS), and it was incubated at room temperature for 10 min before fixation. For strong permeabilizing, 0.1% Triton X-100 was used instead of saponin in the detergent buffer, and incubation was done at room temperature for 3 min. Further fixation and embedding procedures were performed as described above.

## Immunoelectron Microscopy

38 h after infection, Sf9 cells infected with L virus were washed briefly with PBS. Cells were then permeabilized by incubation in a detergent buffer (0.05% saponin and 2 mM GTP in PEM buffer) for 10 min. Cells were collected by mild centrifugation, and they were resuspended in a fixative containing 2% paraformaldehyde, 0.1% glutaraldehyde, 0.05% saponin, and 2 mM GTP based in PEM buffer. After 30 min incubation in the fixative, cells were washed twice with PBS and quenched by incubation in 1 mg/ml NaBH₄ for 10 min. After this, cells were repermeabilized in 0.1% Triton X-100 in PBS for 10 min. Blocking was done by incubating the cells in 5% BSA in PBS. Polyclonal antibody against NF-L (CMN AB 1983) was used at a working dilution of 1:40 as primary antibody. Cells were incubated with the primary antibody at 37°C for 1 h. After incubation, the cells were washed with PBS for 10 min three times, followed by washing in TBS for 10 min three times. Blocking for the second antibody was done in TBS, pH 8.2, including 5% BSA. Colloidal gold–conjugated goat anti-rabbit IgG (Amersham) was used for the second antibody. The antibody was diluted to 1:20 in blocking solution, and it was centrifuged at 6500 rpm for 15 min before use. Second antibody incubation was done at 4°C overnight with mild shaking, and it was then transferred to room temperature and further incubated with mild shaking for 1 h. Then the cells were washed with TBS for 10 min three times and postfixed with 3% glutaraldehyde for 20 min at room temperature. Further osmification and embedding were done as described above.

## Quick-freeze, Deep-Etch Electron Microscopy

2 d after infection, Sf9 cells were briefly washed in PBS, centrifuged at 700 rpm in a swing rotor for 3 min, and the pellets were resuspended in PEM buffer including 0.05% saponin and 2 mM GTP for 10 min at room temperature. Permeabilizing in PEM buffer instead of PBS was a milder condition for Sf9 cells. Then the cells were collected by centrifugation and fixed with PEM buffer including 0.05% saponin, 2 mM GTP, and 2.5% glutaraldehyde for 15 min at room temperature. Collected again by centrifugation, the fixed cells were briefly washed with distilled water and quickly frozen by liquid helium as described previously (Hirokawa and Heuser, 1981).

Fracture was done at −170° and deep etched at −95°C for 7 min either in a Balzers 301 unit or 400 unit (Balzers Union, Fürtentum, Liechtenstein). Platinum and carbon were rotary shadowed, and the replicas were viewed either with a JEOL 1200EX or 2000EX electron microscope at 100 kV. Three-dimensional images were taken with ±10° tilt.

## Measurements of Cross-bridges

Cross-bridges that formed between neurofilaments were measured on quick-freeze, deep-etch images. We used two criteria for the measurement. First, only cross-bridges in the same focus planes, as judged from the three-dimensional images, were counted. Second, only cross-bridges linking two filaments organized in a nearly parallel manner were counted.

## Results

### Absence of Intermediate Filaments in Sf9 Cells

Since neurofilament proteins have a molecular motif that is conserved among intermediate filaments, they tend to coassemble with endogenous intermediate filaments such as vimentin when they are transfected into cultured cells (Chin and Liem, 1989; Monterio and Cleveland, 1989; Wong and Cleveland, 1990; Chin et al., 1991). The ideal condition for

studying neurofilaments would be to get rid of those endogenous intermediate filaments. One choice is to use vimentin (−) fibroblasts (Ching and Liem, 1993; Lee et al., 1993). The other is what we are reporting here. Sf9 cells, an insect ovarian cell line, are derived from IPLB-Sf21 cells that were originally established from *Spodoptera frugiperda*. Antibodies to most of the intermediate filament proteins, including keratins, neurofilament triplet proteins, glial fibrillary acidic protein, desmin, vimentin, and a *Drosophila* vimentin–like protein, did not stain IPLB-Sf21 cells (Volkman and Zaal, 1990). It is well known that crustaceans do not have intermediate filaments (Hirokawa, 1986; Hirokawa and Yorifuji, 1986; Viancour et al., 1987). Classified in the same arthropods, *S. frugiperda*, or Sf9 cells, may not have any intermediate filaments. To confirm this, we searched for intermediate filaments in Sf9 cells by electron microscopy. Sf9 cells were either directly fixed (Fig. 1 *A*) or permeabilized before fixation to get clear views of the cytoskeleton (Fig. 1 *B*). By precipitating fixed Sf9 cells at the tip of the embedded block, we were able to observe more than 100 cells within a single ultrathin section sample. Even though there were microtubules (Fig. 1 *A, arrows*), we were not able to find intermediate filaments.

To further support these findings, we searched for gene transcripts containing a consensus amino acid sequence found in a large number of intermediate filament proteins. This consensus sequence (YRKLLEGEE) is called IFA epitope for its reactivity to the IFA antibody (Pruss et al., 1981), and it resides in the carboxyl-terminal end of the rod domain. Some invertebrates, however, are known to have IFA-negative intermediate filament proteins, which later turned out to be a single amino acid substitution of arginine (R) by a lysine (K) in the same consensus sequence (Reimer et al., 1991). To detect both IFA-positive and -negative intermediate filament gene transcripts in Sf9 cells, we made a synthetic oligonucleotide that anneals with this intermediate filament consensus sequence of the mRNA and, using this oligo as a primer, we synthesized first-strand cDNA with ³²P-labeled dCTP from 500 ng of total poly(A)⁺ RNA. The radioisotope labeled reverse-transcribed (RT) product was resolved in 1% agarose alkaline denature gel and transferred onto a nylon membrane. By exposing this membrane to a FUJI BAS 2000 image analyzing plate, we were able to detect intermediate filament consensus sequence positive first-strand cDNA. Since many intermediate filaments have approximately the same length in nucleotide from the start codon to the carboxyl-terminal end of the rod domain, if there were any mRNA bearing the consensus sequence, the RT product of these may appear as bands ~1.4–1.6 kbp. Indeed, as shown in Fig. 1 *C*, the RT product of poly(A)⁺ RNA from mouse brain formed bands at appropriate lengths, but poly(A)⁺ RNA from Sf9 cells showed only weak signals. Although the IFA antibody does not stain the nucleus in immunofluorescence (Pruss et al., 1981), nuclear lamins of some species have the IFA epitope sequence, and they are recognized by the antibody in Western blots (Osborn and Weber, 1987). So the weak signals in lane 2 may be the nuclear lamins. Thus, by this first-strand cDNA synthesis assay, we were not able to detect intermediate filament consensus sequence positive gene transcript in Sf9 cells. In addition, Sf9 cells were not stained with IFA antibody in immunofluorescence, as shown in the background of the confocal images in Fig. 10.
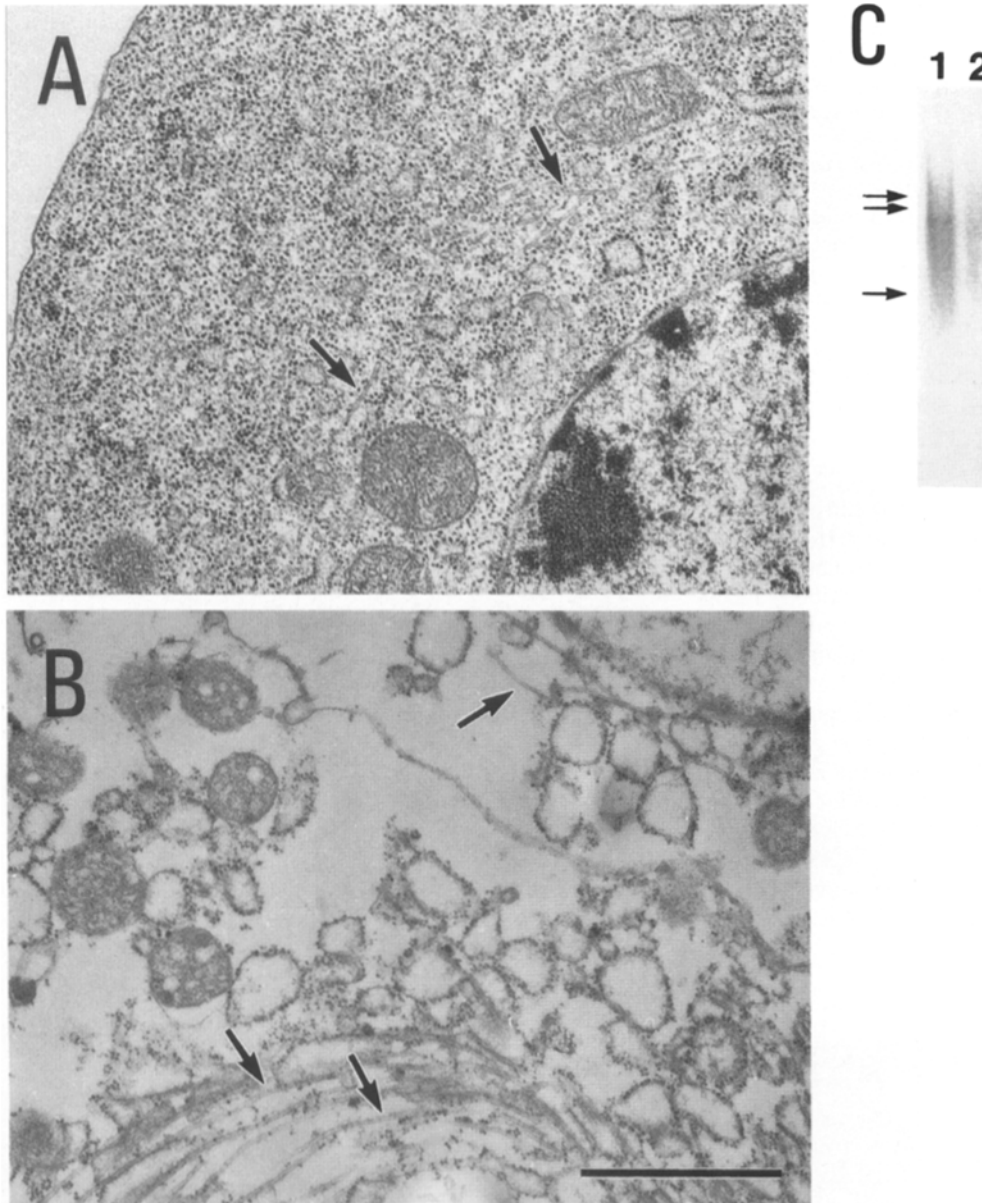
*Figure 1.* Electron micrographs of ultrathin sections of uninfected Sf9 cells. Healthy Sf9 cells were fixed directly (*A*) or permeabilized with 0.05% saponin before fixation (*B*) to get a clear view of the cytoskeletons. More than 100 cells were observed, but we were not able to find any intermediate filaments in the cytoplasm. Microtubules were easily observed (*arrows*). Bar, 1 $\mu$m. 500 ng of poly(A)$^+$ RNA purified from brain was reverse transcribed using a primer that anneals with the intermediate filament consensus sequence in mRNA. This sequence resides at the carboxyl-terminal end of the rod domain. [$^{32}$P]dCTP was incorporated to detect the newly synthesized first-strand cDNA. The RT products were run on 1% agarose alkaline denature gel and transferred onto a nylon membrane for autoradiography. Since all intermediate filaments have approximately the same nucleotide length from the beginning of the head domain to the end of the rod domain, if there are any mRNAs that possess the intermediate filament consensus sequence, RT cDNA bands should appear between 1.4 and 1.6 kbp. Indeed, the RT product of poly(A)$^+$ RNA from brain formed bands $\sim$1.6 kbp (*C*, lane *1*) while poly(A)$^+$ RNA purified from Sf9 cells by the same method did not (*C*, lane *2*) This indicates that in Sf9 cells there are only trace amounts of mRNA bearing the intermediate filament consensus sequence. Arrows on the left indicate 2332, 2027, and 564 bp from the top.

Taking all these together, we propose that Sf9 baculovirus system is another ideal system for studying intermediate filaments. In addition, baculovirus expression vectors promise high level expression, and they are capable of expressing two different proteins by a single virus if desired. This makes the studies of heteropolymers by electron microscopy much easier because the expression of both proteins is guaranteed in infected cells.

## NF-L and NF-M Coassemble and Reproduce the Ultrastructure of Neurofilaments When Transfected into Sf9 Cells
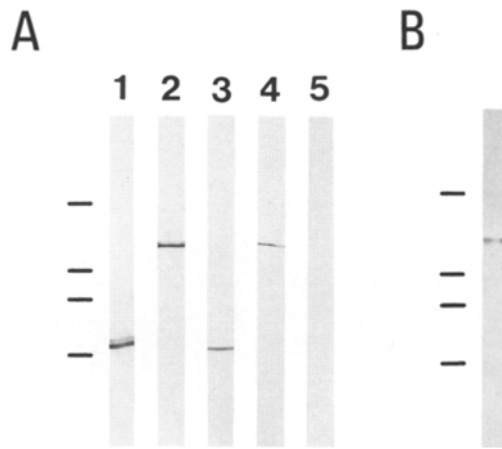
To examine what kind of structures are formed with the expression of NF-L and NF-M and how they are related to the structures of neurofilaments in axons, we transfected both proteins together into Sf9 cells. Three different recombinant baculoviruses were produced. L virus encodes NF-L, LM virus encodes both NF-L and NF-M in a single virus, and M virus encodes NF-M. The profiles of the viruses are listed in Table I. The expression of each protein was checked by Western blotting (Fig. 2 *A*). All viruses expressed the expected proteins at correct molecular weights. Sf9 cells that were not infected with any of the viruses were probed for the antibody used in this study to be sure that no endogenous protein in Sf9 cells cross-reacted with the antibodies (Fig. 2 *A*, lane *5*).

| Names of recombinant baculoviruses | Expressing genes and their promoters |
|---|---|
| L virus | Mouse NF-L; polyhedrin promoter |
| M virus | Rat NF-M; polyhedrin promoter |
| L + M virus | Mouse NF-L; polyhedrin promoter<br>Rat NF-M; p10 promoter |
| L + DelM1 virus | Mouse NF-L; polyhedrin promoter<br>DelM1; p10 promoter |
| L + DelM2 virus | Mouse NF-L; polyhedrin promoter<br>DelM2; p10 promoter |
| L + DelM3 virus | Mouse NF-L; polyhedrin promoter<br>DelM3; p10 promoter |
| L + DelM4 virus | Mouse NF-L; polyhedrin promoter<br>DelM4; p10 promoter |
| L + DelM5 virus | Mouse NF-L; polyhedrin promoter<br>DelM5; p10 promoter |
| L + Mmyc virus | Mouse NF-L; polyhedrin promoter<br>NF-Mmyc; p10 promoter |
| L + DelM1 myc(−) virus | Mouse NF-L; polyhedrin promoter<br>DelM1 myc(−); p10 promoter |



*Figure 2.* Western blot analysis of the recombinant baculovirus product. (*A*) NF-L and NF-M expressed by the virus vectors were recognized by the appropriate antibodies. Total homogenates from Sf9 cells infected with L virus (lane *1*), M virus (lane *2*), and LM virus (lanes *3* and *4*) were resolved on 7.5% SDS polyacrylamide gel, transferred onto a nitrocellulose filter, and blotted with anti–NF-L antibody (lanes *1* and *3*) and anti–NF-M antibody (lanes *2* and *4*). Lane *5* was loaded with noninfected Sf9 cell total homogenates and probed against the two antibodies to show that they do not cross-react with other endogenous proteins in Sf9 cells (*B*) Total homogenates of M virus–infected cells were blotted against an antibody (SMI31) that recognizes the phosphorylated form of the carboxyl-terminal tail of NF-M. This Western blot indicates that NF-M expressed in Sf9 cells is phosphorylated correctly to a certain extent. Bars on the left indicate molecular mass markers: 200, 116, 97, and 66 kD from the top.

The quality of the expressed NF-M was further checked by probing against the anti–phosphorylated NF-M monoclonal antibody SMI 31 (Sternberger and Sternberger, 1983; Lee et al., 1988; Harris et al., 1991). This antibody recognizes amino acid sequences in the carboxyl-terminal tail domain of NF-M that are known to be phosphorylated. As shown in Fig. 2 *B*, SMI 31 recognizes NF-M expressed in the Sf9 baculovirus system. Thus, in Sf9 cells, phosphorylation seems to be occurring at this site.

Each recombinant virus starts to express the foreign gene product ∼10 h after infection. The expression increases with time, but degradation of the protein then starts at ∼50 h after infection for some unknown reason. We chose 38 h after infection as the best time for analyzing neurofilament assembly because at this point, there is already sufficient protein expressed so that the structure desired for observation by elec-

tron microscopy will be available, and because, most importantly, the intracellular structure of Sf9 cells is still well maintained at this moment.

First we observed the neurofilaments by immunofluorescence. Sf9 cells are spherical cells that easily detach from the culture dish. No change in this apparent spherical mor-
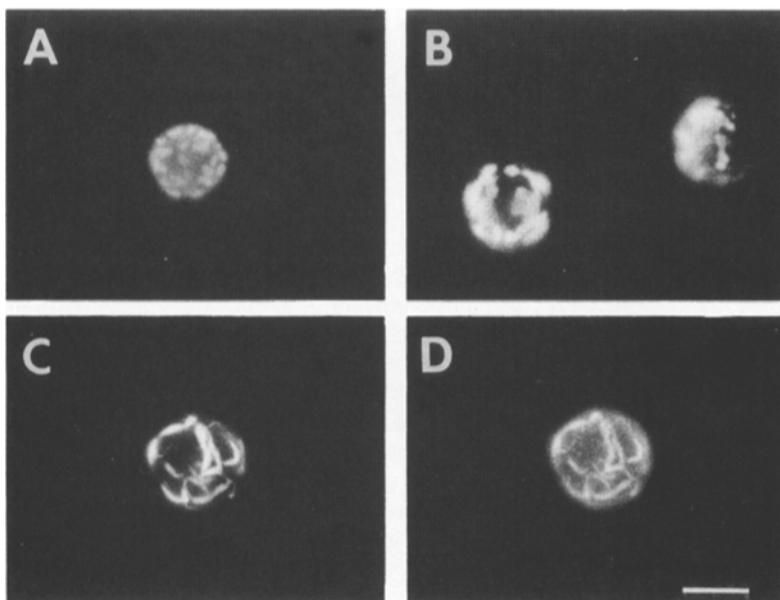


*Figure 3.* Immunofluorescence of transfected Sf9 cells. Sf9 cells infected with L virus (*A*), M virus (*B*), and LM virus (*C* and *D*) were stained with neurofilament antibodies (anti–NF-L monoclonal antibody for *A*; anti–NF-L polyclonal antibody for *C*; anti–NF-M monoclonal antibody for *B* and *D*) to observe the intracellular distribution of the transfected proteins. When either NF-L or NF-M was transfected alone in Sf9 cells, neither showed filamentous staining patterns. On the other hand, when both NF-L and NF-M were transfected together, they colocalized and appeared as thick, filamentous cables, as shown by double staining of LM virus–infected cells with anti–NF-L and anti–NF-M antibodies (*C* and *D*). Bar, 10 μm.

phology was induced by transfecting neurofilament proteins. When NF-L was expressed alone no filamentous staining appeared. Rather, many spotty clusters were observed (Fig. 3 A). In contrast, when both NF-L and NF-M were transfected by the LM virus thick filamentous cables were observed (Fig. 3, C and D). Both proteins colocalized onto these cables, as revealed by double staining. To rule out the possibility that these filament cables are formed by interaction between NF-M and some unexpected protein that preexists in Sf9 cells, we also expressed NF-M alone by infecting M virus as a control. In this case, huge masses stained with anti–NF-M were observed, and no filamentous patterns appeared (Fig. 3 B). Thus, we conclude that the filamentous stainings in LM virus infection are caused by the interaction between NF-L and NF-M.

To identify the ultrastructure of the staining observed by immunofluorescence, we investigated these structures by electron microscopy. Cells infected with the L virus showed either a complicated random network of 10-nm filaments or tightly packed aggregates (Fig. 4 A) By permeabilizing the infected cells with 0.1% Triton X-100 before fixation we were able to clearly visualize fragments of 10-nm filaments in the random network, but the aggregates remained unchanged (Fig. 4 B). Immunoelectron microscopy proved that these structures were indeed formed by NF-L (Fig. 5 A). We further viewed the random network formed by NF-L by quick-freeze, deep-etch electron microscopy to confirm that no cross-bridges were formed (Fig. 5 B).

Interestingly, in contrast, Sf9 cells infected with LM virus showed parallel bundles of 10-nm filaments with approximately constant spacing in ultrathin sections (Fig. 4 E). Even when permeabilized with 0.05% saponin in phosphate buffer before fixation, these ordered structures were preserved, indicating that the force acting between the filaments is not so weak (Fig. 4 F). Faint cross-bridge–like structures could be seen, even in the ultrathin sections. Quick-freeze, deep-etch electron micrographs provided further detailed information (Fig. 6, A and B). Frequent cross-bridges were observed between core filaments organized in a parallel manner. This ultrastructure formed by transfected NF-L and NF-M highly resembled neurofilament domains in axons (Fig. 6 C). In some cases, cross-bridges between membranous organelles and neurofilaments were also seen in transfected cells (Fig. 6 B, arrows). This kind of cross-bridge was not observed in L virus–infected cells. On the other hand, in Sf9 cells infected with M virus alone, only aggregates were observed, while no 10-nm filaments were formed (Fig. 4 C). These aggregates were not dissociated by permeabilizing these cells with 0.1% Triton X-10 before fixation (Fig. 4 D). Thus, NF-M alone cannot form 10-nm filaments in vivo.

These data strongly indicate that the interaction between NF-L and NF-M is absolutely required to form parallel neurofilament arrays linked to each other with frequent cross-bridges as seen in axons, and that some cross-bridges between membranous vesicles and neurofilaments in vivo are formed by NF-M. Also, this parallel array was not disrupted by permeabilization, which suggests an active bundling effect caused by these cross-bridges. The stoichiometry between NF-L and NF-M expressed by LM virus was measured by analyzing SDS-PAGE of the cytoskeletal fraction of infected cell lysates in PDI densitometry, giving the value NF-L/NF-M = 1:0.7.

## Myc Tags of Carboxyl Terminal Tail Domain of NF-M Do Not Affect Cross-bridge Formation upon Neurofilament Assembly

Similarity in the molecular architecture of NF-H and NF-M suggests that the carboxyl-terminal tail domain of NF-M constitutes cross-bridges, as is the case for NF-H. Even though there are many descriptive data supporting this idea, so far no direct evidence has been provided. To present such direct evidence that the carboxyl-terminal tail domain of NF-M is actually involved in cross-bridge formation, we made five deletion mutants of NF-M that lack part of the tail domain (Fig. 7). By expressing these deletion mutants with NF-L, the ability to form 10-nm filaments and the assembling property were examined. We conjugated a human myc epitope in the carboxyl-terminals of each deletion mutant to facilitate detection by immunofluorescence. Although many transfection experiments of neurofilaments have used similar kinds of epitopes, the effect of the artifact of these tags upon neurofilament assembly has not been fully evaluated. Thus, as a sixth mutant, we fused this myc epitope tag in the carboxyl-terminal of full-length NF-M and named it Mmyc. L + Mmyc virus, which encodes NF-L and Mmyc in a single virus, was infected into Sf9 cells, and the filament assembly properties were compared with wild-type NF-M.The expression of both proteins was confirmed by Western blotting (data not shown). Immunofluorescence microscopy double stained with anti–NF-L antibody and anti–myc epitope antibody (Fig. 7, inset) shows that they colocalize to form similar cable-like stainings as observed in wild-type NF-L + NF-M (Fig. 3). Quick-freeze, deep-etch views of the filaments assembled by NF-L and Mmyc (Fig. 7) are almost identical to those formed by wild-type NF-L + NF-M (Fig. 6, A and B), and they are similar to those in axons (Fig. 6 C). Core 10-nm filaments running in parallel and forming bundles are observed, and frequent cross-bridges exist between these filaments. The lengths of the cross-bridges were measured and compared with those formed by wild types (see Fig. 12). We did not detect any significant difference between them. Thus, the human myc epitope tag linked in the carboxyl-terminal did not interfere with cross-bridge formation.

## Deletion Mutants of NF-M Lacking Part of the Carboxyl-terminal Tail Domain Colocalize with NF-L When Expressed in Sf9 Cells

Five deletion mutants of NF-M were constructed (Fig. 8). All mutants were expressed by recombinant baculoviruses in a manner that both NF-L and mutant NF-M were expressed by a single virus. Profiles of the viruses are listed in Table I. Expression of each protein was confirmed by Western blotting (Fig. 8 B). Mutant NF-Ms with myc tags in the carboxyl-terminals were detected by anti–human myc epitope antibody. NF-L was detected by anti–NF-L antibody. All proteins were recognized by the appropriate antibodies without any cross-reaction (Fig. 8). The expression of each protein starts at least 12 h after infection. As in the case for wild-type NF-L and MF-M, partial degradation of some of the proteins starts at ~50 h after infection. We decided to analyze cells at 38 h after infection since high level expression and well-preserved intracellular structures can be obtained at this point.

Double staining immunofluorescence microscopies of Sf9

Nakagawa et al. NF-M and Neurofilament Assembly In Vivo

417

418
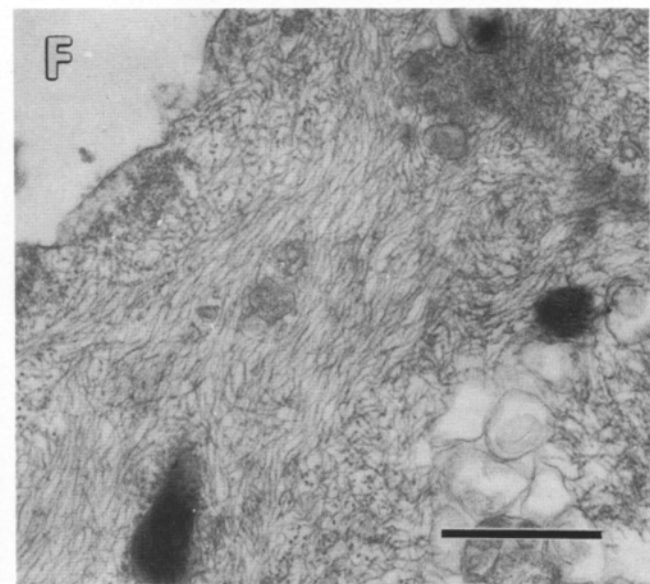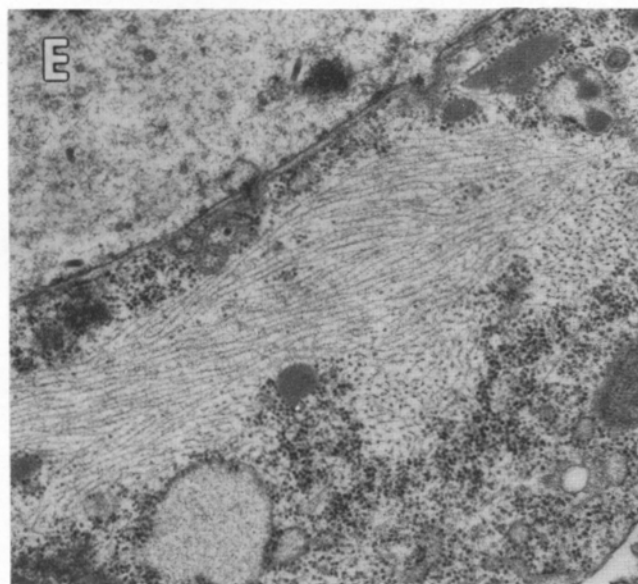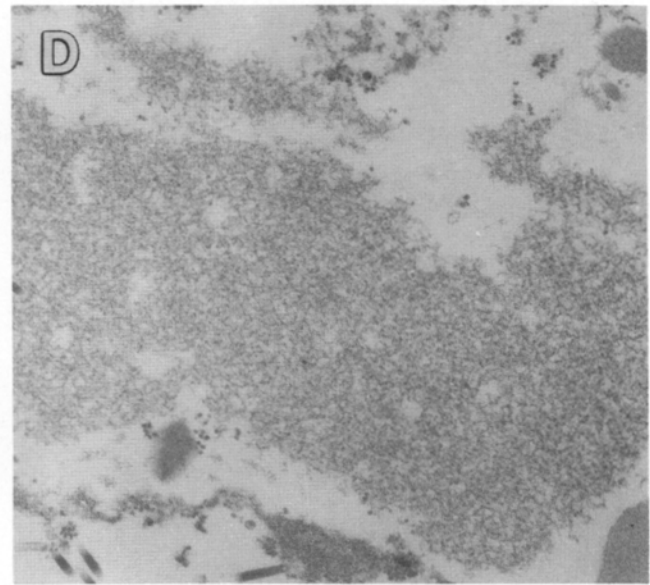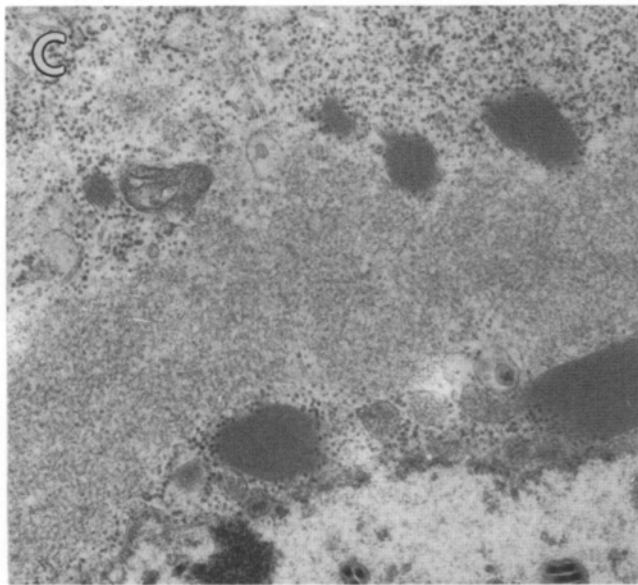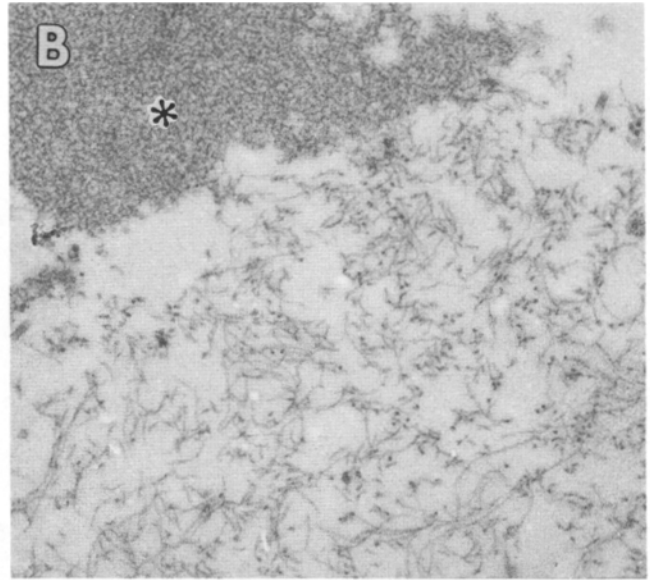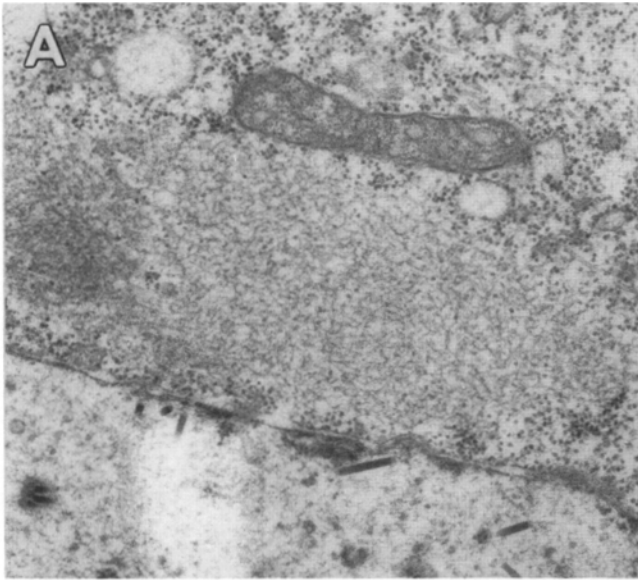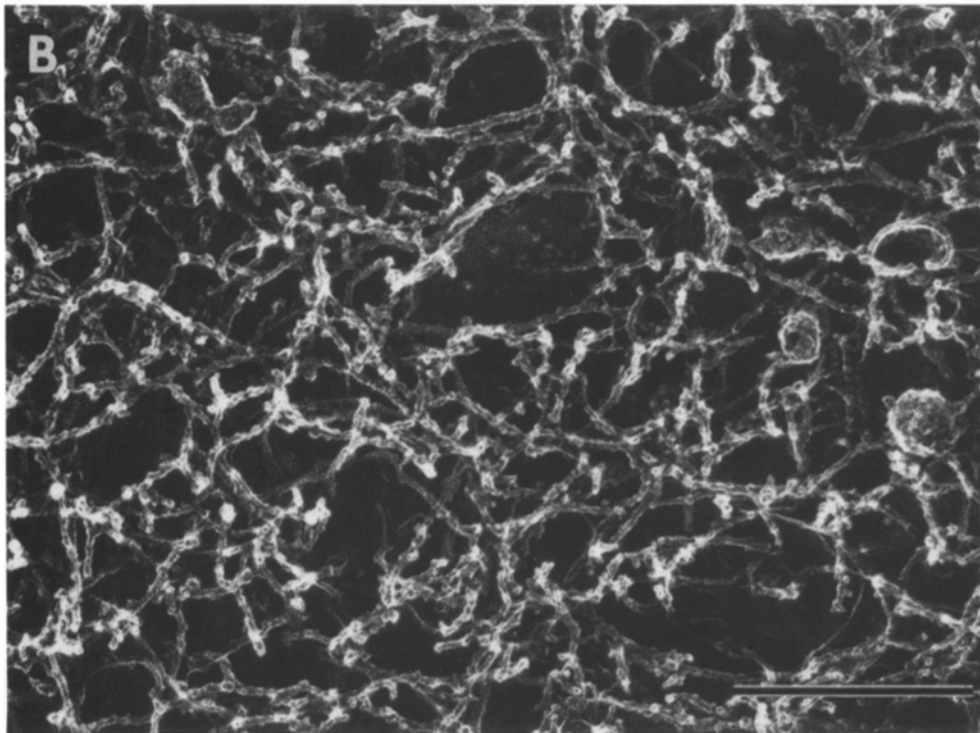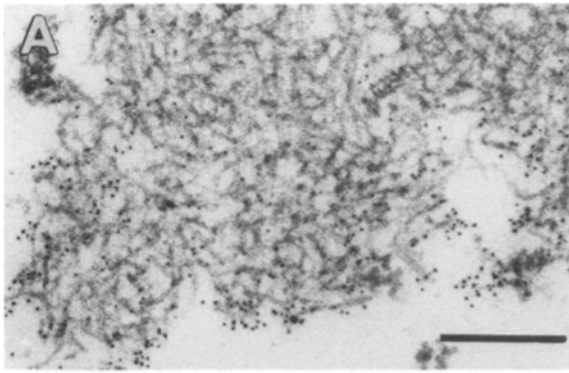
*Figure 5.* To confirm that the filaments observed in Fig. 4, *A* and *B*, are indeed formed with transfected NF-L, immunoelectron microscopy study was done (*A*). Sf9 cells infected with L virus were incubated with a primary antibody against NF-L and further incubated with colloidal gold–conjugated secondary antibody. As shown in *A*, the clusters formed of short fragmented filaments were strongly labeled with colloidal gold particles. Bar in *A*, 200 nm. (*B*) A quick-freeze, deep-etch view of Sf9 cells transfected with NF-L (corresponding to the ultrathin section viewed in Fig. 1, *A* and *B*) is shown. NF-L polymerizes into short fragmented filaments that are coordinated in a random manner, forming loose networks. No cross-bridge structures were observed between the adjacent filaments. The surface of each filament was not smooth or, in other words, was very irregular. Bar in *B*, 400 nm.

cells infected with each virus show that both NF-L and mutant NF-Ms co-localize to restricted areas in each cell (Figure 9). Clear cables of filaments in the staining patterns, however, were not observed in any of the cases. In some cells, filament-like staining was observed by moving the focus plane, indicating that filaments are probably formed within these stainings. These immunofluorescence studies showed that the whole carboxyl-terminal tail domain of NF-M is required for effective bundling of neurofilaments. The quantity of NF-L expressed in these cells exceeds that of mutant NF-Ms. The stoichiometry between NF-L and

mutant NF-Ms expressed by each virus was measured by densitometry analysis of the cytoskeletal fraction resolved in SDS-PAGE (Table II). L + *Mmyc* virus expresses NF-L approximately four times more than *Mmyc* in molar quantity but it still retains the filament cable staining pattern. This means that stainings of the deletion mutant–expressing cells are not simply caused by the greater amounts of NF-L compared to deleted NF-Ms.

Constructs similar to DelM1 were used in previous transfection studies (Ching and Liem, 1993; Lee et al., 1993), and they were shown by immunofluorescence to distribute

*Figure 4.* Electron micrographs of transfected Sf9 cells. In Sf9 cells infected with L virus, which expresses NF-L, clusters of short, fragmented filaments were observed in the cytoplasm (*A* and *B*). In some cases, transfected NF-L made aggregates (*B, asterisk*). To get a clearer view of the filaments formed, we permeabilized the infected cells before fixation with 0.1% Triton X-100 (*B* and *D*). (*C* and *D*) Electron micrographs of Sf9 cells infected with M virus, which expresses NF-M. NF-M aggregated when expressed alone in these cells and no 10-nm filaments were observed. When both NF-L and NF-M were expressed together by infecting the cells with LM virus, parallel arrays of 10-mm filaments were observed in the cytoplasm (*E*). As shown in *F*, this parallel array was not disrupted, even when the cells were permeabilized with 0.05% saponin before fixation. Bar, 600 nm.
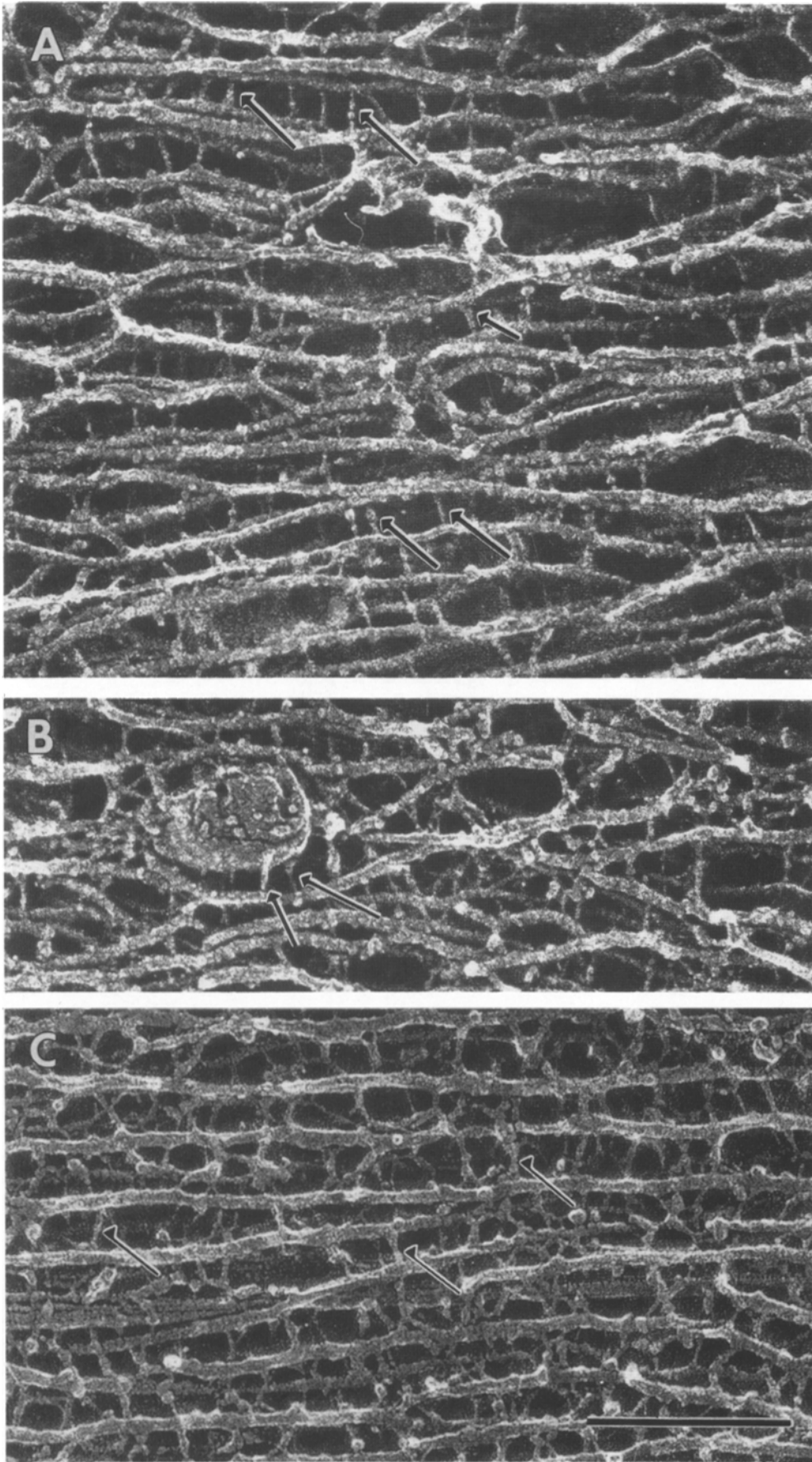
*Figure 6.* Quick-freeze, deep-etch view of the filaments formed by NF-L and NF-M in LM virus infected Sf9 cells (*A* and *B*). These correspond to the ultrathin section view in Fig. 4, *E* and *F.* Between the parallelly arranged 10-nm filaments, frequent cross-bridges were observed (*A, arrows*). Structures formed by the transfected NF-L and NF-M highly resemble neurofilaments in neuronal axons, which are shown in *C* for comparison. The cross-bridges in Sf9 cells, however, are not as frequent as observed in axons. In the axon of rat peripheral nerves treated similarly to the Sf9 cells, neurofilaments run parallel to each other, forming frequent cross-bridges between the adjacent filaments (*C, arrows*). In our transfected cells, cross-bridges between filaments and membranous organelles were also observed (*B, arrows*). Bar, 200 nm.
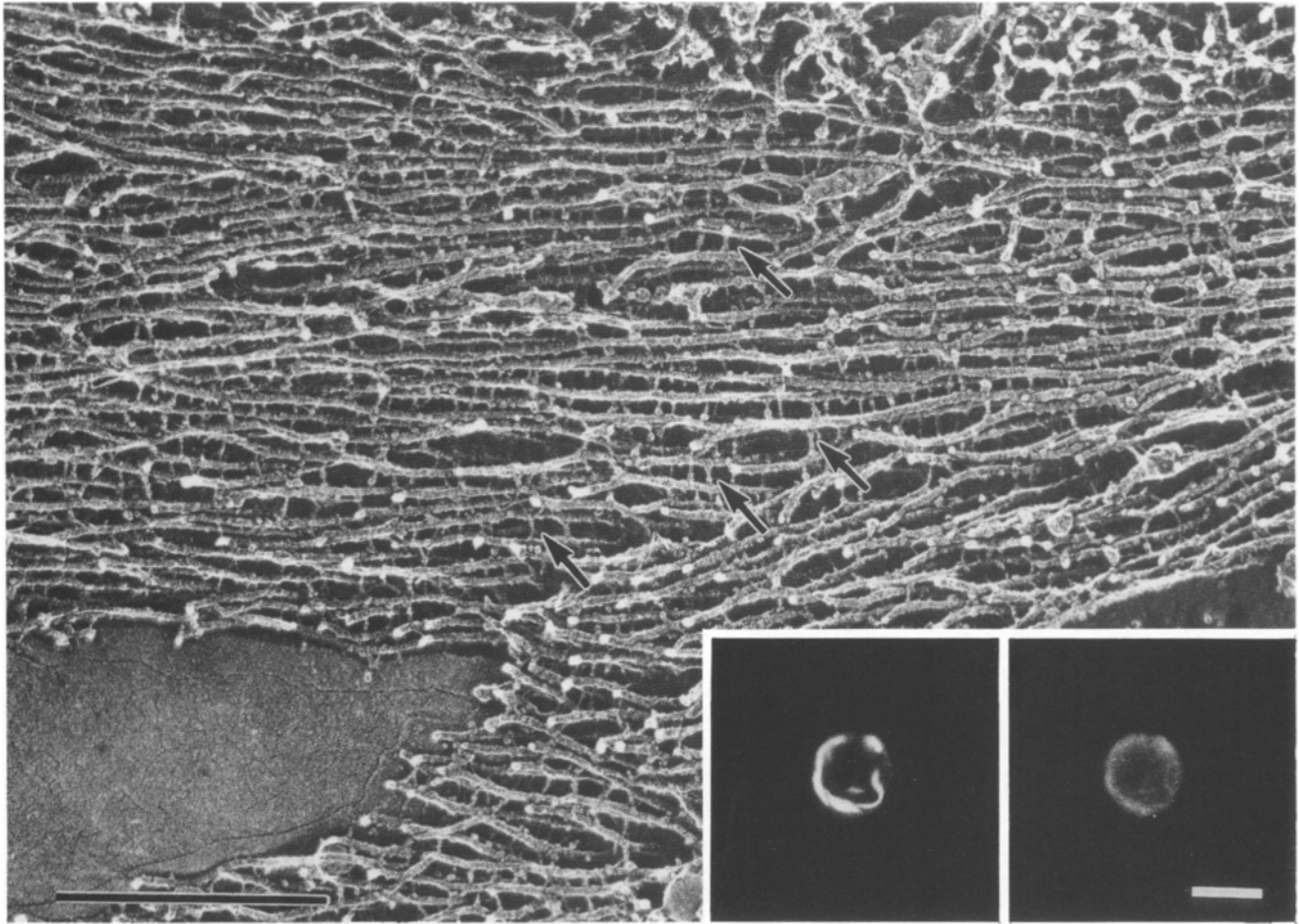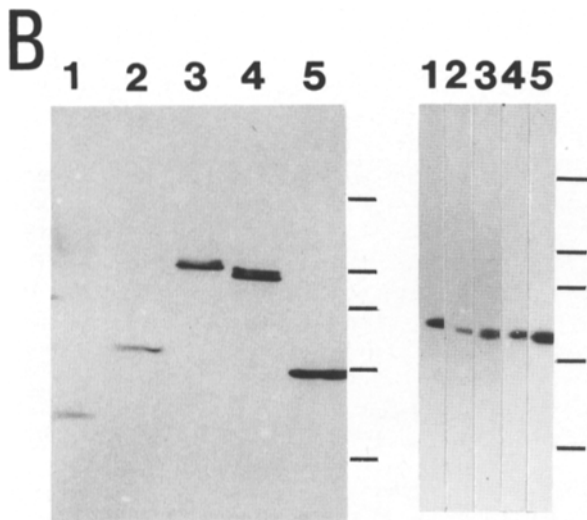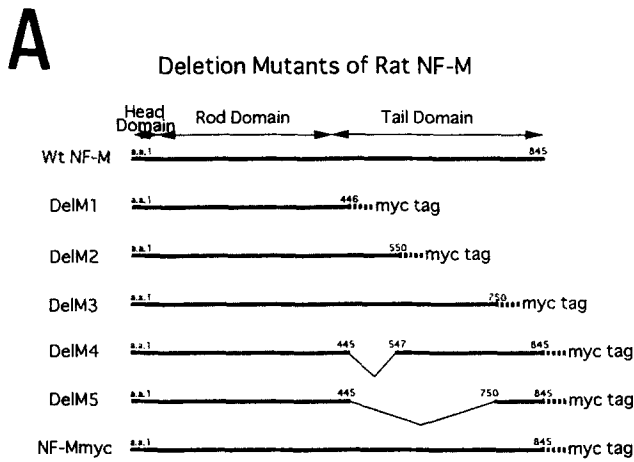
*Figure 7.* Quick-freeze, deep-etch view of the filaments formed by NF-L and NF-*Mmyc* in L + *Mmyc* virus–infected Sf9 cells. The three-dimensional ultrastructure of the filaments formed show no significant change compared to those formed by NF-L and wild-type NF-M. Filaments running parallel to each other formed frequent cross-bridges (*arrows*) between the adjacent filaments. Double staining immunofluorescence micrographs of these cells are shown in the inset. Anti–NF-L polyclonal antibody (*right*) and anti-*myc* epitope monoclonal antibody (*left*) were used as primary antibodies. Both proteins colocalize and form thick filamentous cable staining. From these results, *myc* tag linked at the carboxyl-terminal of NF-M has little, if any, effect on filament assembly or cross-bridge formation. Bar in the electron micrograph, 500 nm; bar in the immunofluorescence micrograph, 10 $\mu$m.

within cells in filamentous staining colocalizing with NF-L. Although this apparent filamentous staining was not observed in our experiment, these stainings were revealed to be tightly packed 10-nm filaments, as viewed by electron microscopy (details of which appear later in this paper). Lee et al. (1993) used a *myc*-tagged deletion mutant similar to

*Table II. Measurements of Deletion Mutant Analysis*

| Virus | Expression levels in molar ratio | Length of cross-bridges (length ± SEM nm) |
|---|---|---|
| L + M | L:M = 1:0.75 | 31.57 ± 0.56 |
| L + DelM1 | L:DelM1 = 1:0.60 | No cross-bridges |
| L + DelM2 | L:DelM2 = 1:0.39 | 16.46 ± 0.54 |
| L + DelM3 | L:DelM3 = 1:0.23 | 28.12 ± 0.46 |
| L + DelM4 | L:DelM4 = 1:0.18 | 26.43 ± 0.59 |
| L + DelM5 | L:DelM5 = 1:0.40 | No cross-bridges |
| L + Mmyc | L:Mmyc = 1:0.25 | 33.98 ± 0.60 |

DelM1. In their data, filamentous staining was observed only in the periphery of the cell, and the strong staining in the central region, which we consider to be a mass of tightly packed filaments, is noteworthy. In contrast, Ching and Liem (1993) used deletion mutants similar to DelM1, but with no tag. This mutant seems to form bundles of filaments with NF-L in intermediate filament negative fibroblasts observed by immunofluorescence microscopy. The slight difference between the two studies concerning this deletion mutant may be caused by the *myc* tag. Thus, the artifact of the tag would come into question. To exclude the possible artifact of the *myc* tag in DelM1, we constructed another virus that expresses NF-L and DelM1 lacking the tag (L+DelM1 myc(−) virus). We double stained Sf9 cells infected with this virus with anti–NF-L antibody and IFA antibody (Pruss et al., 1981). IFA reacts very weakly with native proteins in Sf9 cells, as seen from the cells in the background in the confocal image (Fig. 10). Western blot of Sf9 cells infected with L+ DelM1myc(−) virus revealed that this antibody specifically

# A

## Deletion Mutants of Rat NF-M



## B



*Figure 8.* Schematic drawings of the deletion mutants of rat NF-M (A). See Materials and Methods for details. *Myc* epitope was attached to the carboxyl-terminal of each mutant as a tag for immunofluorescence microscopy. Small numbers indicate amino acid residues. Each of these mutant NF-Ms was ligated into baculovirus expression transfer vectors to produce the viruses listed in Table I. To check the expression of the recombinant proteins, Western blot analysis of the whole cell homogenates of the cells infected with the five viruses is shown in *B*; L + DelM1 (lane *1*), L + DelM2 (lane *2*), L + DelM3 (lane *3*), L + DelM4 (lane *4*), and L + DelM5 (lane *5*). The left five lanes were blotted against anti-*myc* epitope antibody, and the right five were blotted against anti NF-L antibody. Bars on the right of the two blots indicate molecular mass markers: 200, 116, 97, 66, and 43 kD from the top. All recombinant neurofilament genes encoded by the baculovirus vectors are expressed correctly at the appropriate molecular masses.

recognizes the neurofilaments introduced (data not shown). Bands that correspond to nuclear lamins did not appear in this Western blot (thus, the reactivity of IFA antibody to Sf9 nuclear lamins seems to be weak). Confocal microscopic observation revealed no significant difference between DelM1 with or without the tag (Fig. 10 vs 9 *A*). Stoichiometry of NF-L to DelM1myc(−) was 1:0.3. Taken all together, we could not detect a significant artifact caused by the tag in case of DelM1.
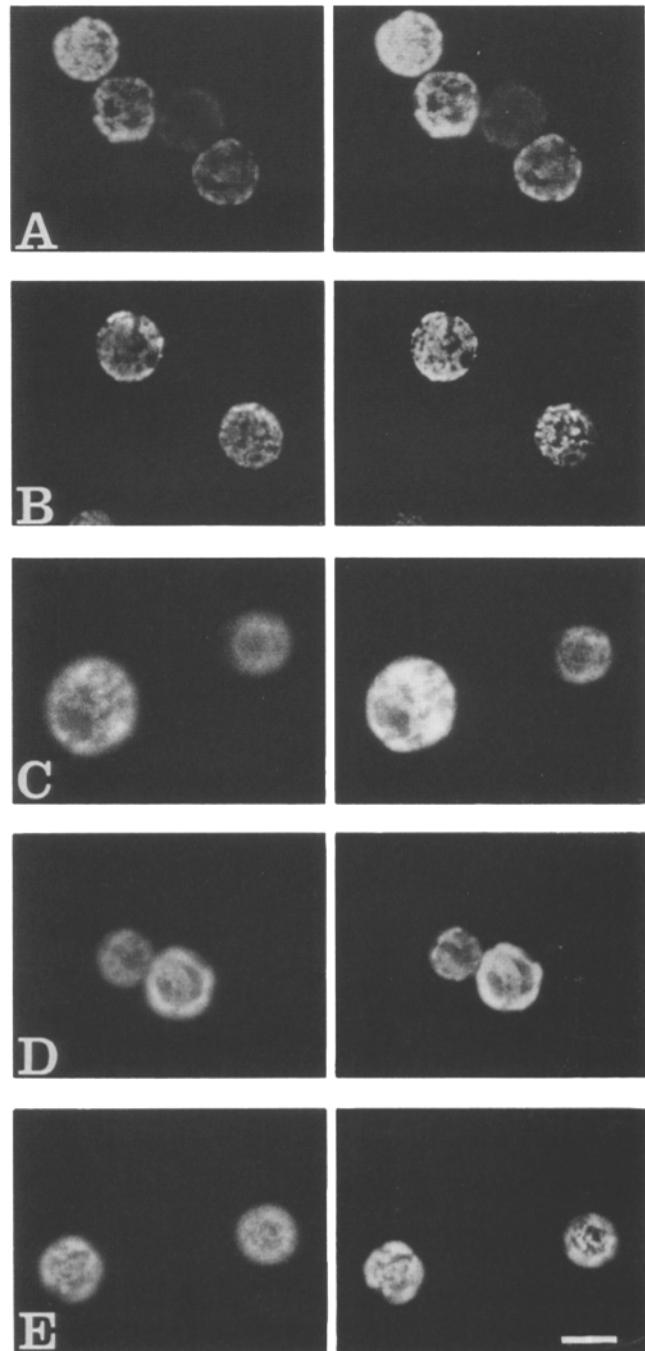


*Figure 9.* Double staining immunofluorescence of the cells infected with the following viruses: L + DelM1 (*A*), L + DelM2 (*B*), L + DelM3 (*C*), L + DelM4 (*D*), and L + DelM5 (*E*). Left panels of each row are the stainings of NF-L and the right panels are of myc epitope attached to the deleted NF-Ms. In all cases, both NF-L and deleted NF-M colocalized within the transfected Sf9 cells, but no thick filamentous stainings, such as those seen in case of NF-L and NF-M double expression (Fig. 3, *C* and *D*), were observed. When observed by electron microscopy, however, these turned out to be masses of filaments in some cases. See text for details. Bar, 10 μm.
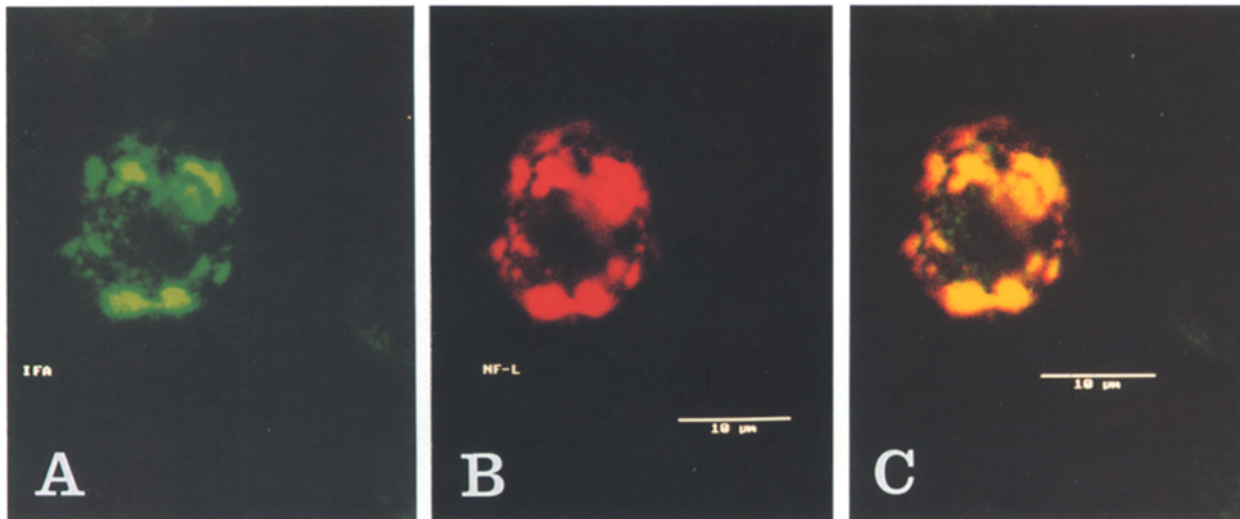
*Figure 10.* Confocal images of Sf9 cells double expressing NF-L and DelM1myc(−). Cells were double stained with anti–NF-L antibody (*B*) and IFA antibody (*A*), which recognize both NF-L and DelM1myc(−). Specificity of IFA was checked by Western blotting to recognize only NF-L and DelM1myc(−) in L + DelM1myc(−) virus–infected cells (data not shown). Overlay image of the NF-L and IFA stainings are shown in *C*. The yellow areas indicate colocalization. Little IFA staining is detected outside NF-L stainings. By observing the focal planes at every 1 $\mu$m, we were not able to detect any filamentous staining patterns. Bars, 10 $\mu$m.

## Cross-bridge Formation Was Strongly Influenced by NF-M Deletion Mutants Lacking Part of Their Carboxyl-terminal Tail Domain

The filament assembly abilities of NF-L with each of the five NF-M deletion mutants in Sf9 cells were further observed by electron microscopy. Ultrathin sections of the infected cells revealed that, even tough they do not make clear bundles NF-L + DelM1, 2, 3, and 4 each assemble into 10-nm filaments, respectively, and NF-L + DelM5 forms aggregates of which the structure is unclear (data not shown). Quick-freeze, deep-etch images of the filaments formed by these transfected proteins are shown in Fig. 11. NF-L and DelM1 assemble to form packed, complicated tangles of 10-nm filaments (Fig. 11 *A*). The tendency of filaments to develop parallel coordination gets stronger as the length of carboxyl-terminal tail domain encoded in the deletion mutants increases. DelM5 formed either filaments similar to DelM1 (Fig. 11 *E*) or compact aggregates (Fig. 11 *F*).

To examine the cross-bridges formed by the coassembly of NF-L and mutant NF-Ms, filaments were viewed by quick-freeze, deep-etch electron microscopy. NF-L and DelM1 did not form clear cross-bridges. On the other hand, NF-L and DelM2 formed cross-bridges that were apparently shorter than those formed by filaments assembled by NF-L + DelM3 or NF-L + DelM4 (Fig. 11 *B–D*). Length of cross-bridges formed in each transfection was determined by statistical analysis (Fig. 12). Cross-bridges in NF-L + DelM2 are shorter than those formed by wild-type or the other deletion mutants. Considering the fact that DelM1 does not form cross-bridges, regions that are in the carboxyl-terminal to amino acid residue 446 are strongly indicated to be directly concerned with cross-bridge formation.

Another noteworthy point is that the cross-bridges formed by these deletion NF-Ms were at surprisingly low frequen-

cies compared to those formed by wild-type NF-M or Mmyc. This can be explained by the fact that interaction between certain regions of the carboxyl-terminal tail domain of NF-M is critical for frequent cross-bridge formation. In search for such interactions, we coinfected L + DelM2 and L + DelM4 to determine if there is significant interaction between the two regions, amino acids 446–550 and 750–845. Immunofluorescence microscopy of these doubly infected cells showed no significant change in the staining pattern (data not shown). Since the interaction between these regions is the only remaining possibility deduced from our deletion mutant analysis, we conclude that the whole-tail domain of NF-M is required for efficient cross-bridge formation and neurofilament bundling.

## The Carboxyl-Terminal Tail Domain of NF-M Promotes Longitudinal Extension of the Core 10-nm Filaments

The three-dimensional organization of the filaments assembled by NF-L and mutant NF-Ms revealed that the assembly properties of the deletion mutants differ significantly. The differences appeared most clearly in quick-freeze, deep-etch views of the filaments. Filaments formed by L + DelM1 and L + DelM5 are frequently bent in a complex manner, and only short fragments of any single filament appear in the fracture surface (Fig. 11, *A* and *E*). In the case of L + DelM5, the filaments aggregate so tightly that single filaments are hardly detectable (Fig. 11 *F*). In contrast, L + DelM2, L + DelM3 and L + DelM4 assemble filaments that are relatively straight and tend to appear as long fragments that could be easily followed in the fracture surface (Fig. 11 *B–D*). In addition, as mentioned before, cross-bridges in these deletion mutants are very rarely seen. The difference of expression stoichiometry between NF-L and

424
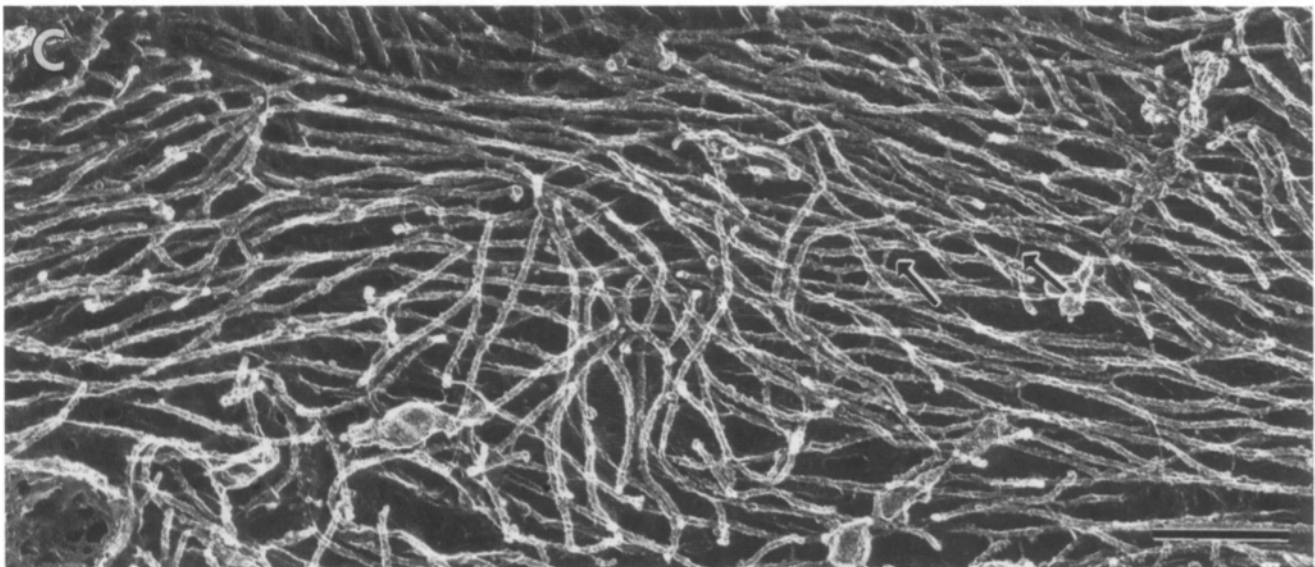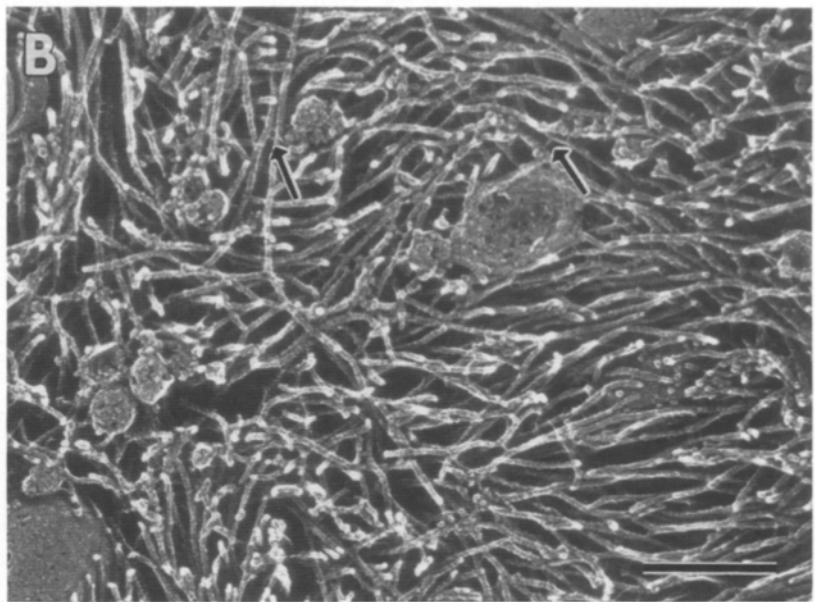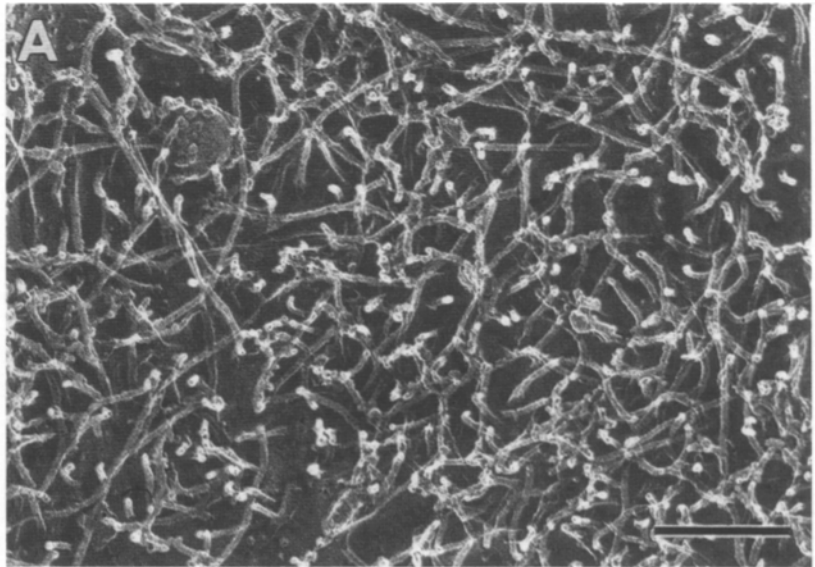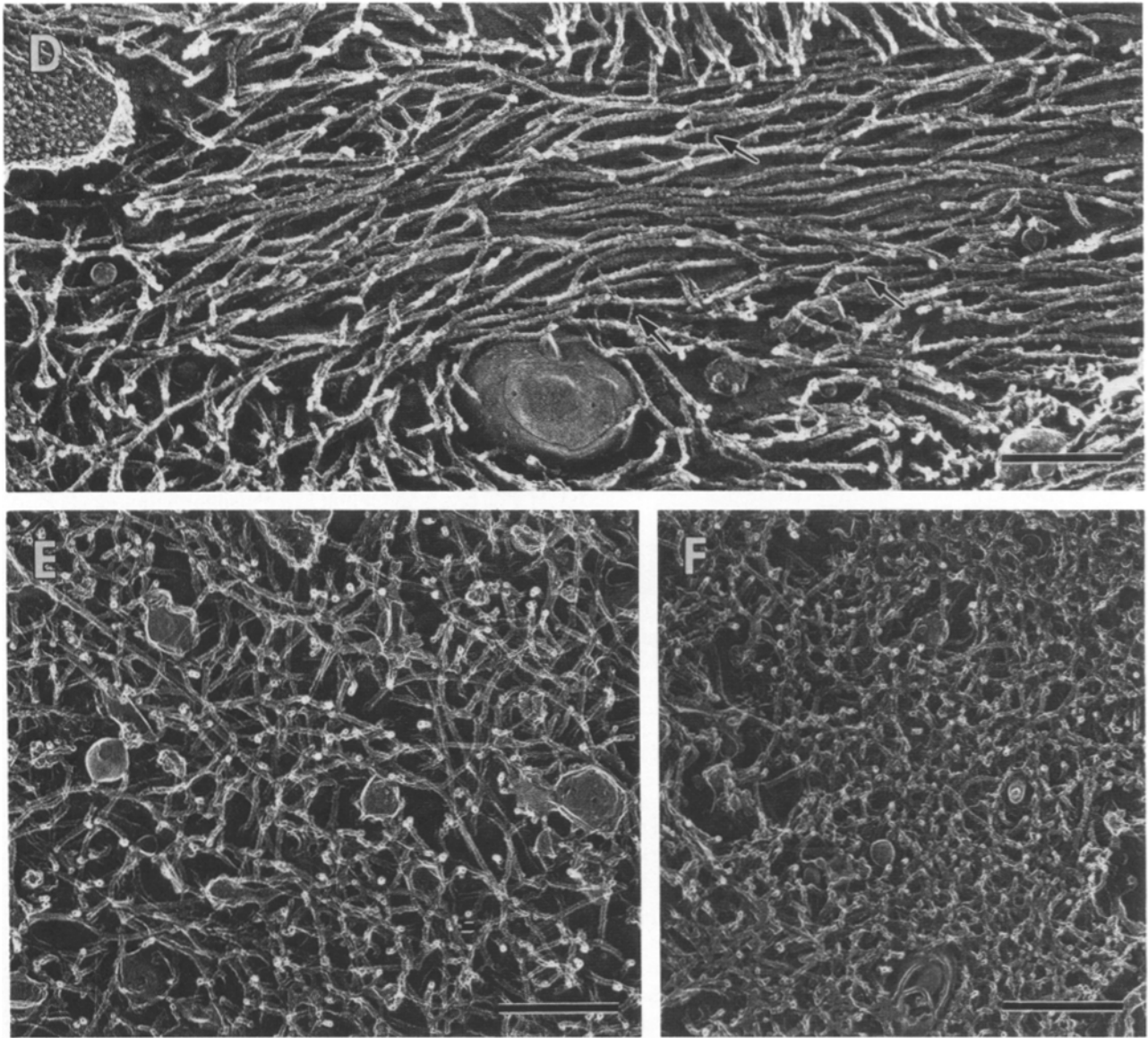
*Figure 11.* Quick-freeze, deep-etch views of the filaments formed by NF-L and the deletion mutants of NF-M. (*A*) L + DelM1-infected Sf9, (*B*) L + DelM2-infected Sf9, (*C*) L + DelM3-infected Sf9, (*D*) L + DelM4-infected Sf9, (*E* and *F*) L + DelM5-infected Sf9. Since DelM1 and DelM5 only form short randomly organized filaments and no cross-bridges with NF-L, we consider that the regions included in the other three deletion mutants are required for effective formation of longitudinally extended filaments with cross-bridges (*arrows*). See text for details. Bars, 270 nm.

mutant NF-Ms (as mentioned in Table II) cannot account for the sparseness of cross-bridges in the respective case. If all mutant NF-M molecules are able to project their carboxyl-tail domain from the core filaments to form cross-bridges, the frequency of these cross-bridges in L + DelM2, L + DelM3, and L + DelM4 should be much higher. Therefore, not all the carboxyl-terminal tail domains of these mutant NF-Ms contribute to form cross-bridges. The population of mutant NF-Ms that do not form cross-bridges seems to affect the core filament assembly property in a manner that longitu-dinal elongation is promoted. This effect of the tail domain on core filament assembly is reflected most clearly by com-paring the quick-freeze, deep-etch view of the filaments formed by the five different deletion mutants (Fig. 11). Since
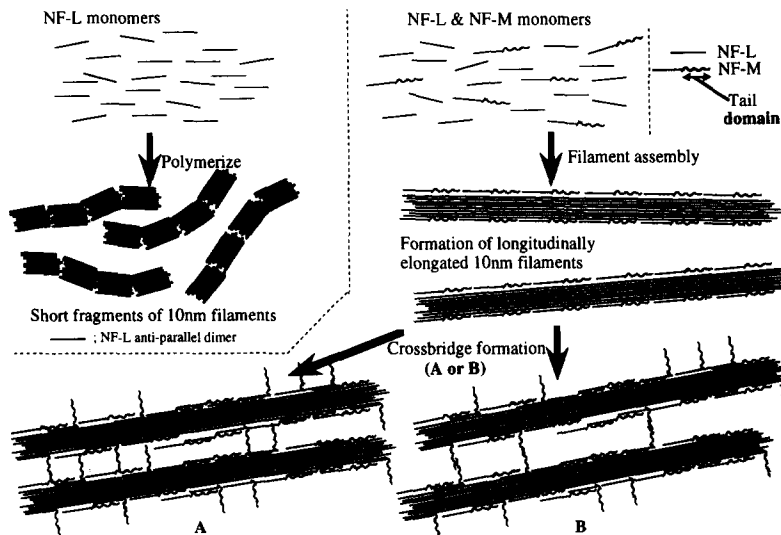
L + DelM1 does not form any cross-bridges, and since the three-dimensional organization of the assembled filaments is much more disordered than those of L + DelM2, L + DelM3, and L + DelM4, the portion of the carboxyl-terminal tail domain of NF-M that is actually involved in cross-bridge formation may promote longitudinal assembly of core filaments by partially associating with the core fila-ments. In this case, the tail domain seems to be sticking to the core filaments without hanging out as projections. Effec-tive formation of cross-bridges is only observed when the whole tail domain exists. Here, we conclude that the function of the carboxyl-terminal tail of NF-Ms is to promote longitu-dinal assembly when they are as yet not hanging out as projections from the core filament, and then, once they de-

## length of crossbridges
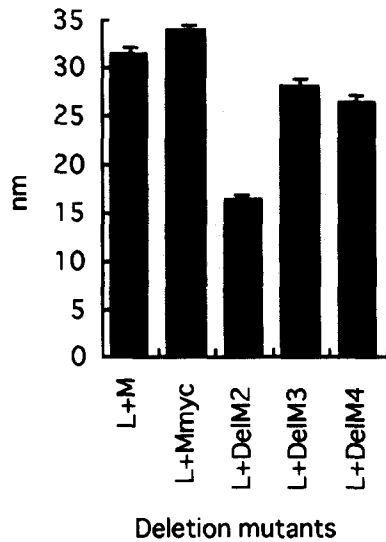


*Figure 12.* Length of cross-bridges formed by wild-type NF-M and mutant NF-Ms were measured. See Materials and Methods for details of procedure. DelM1 and DelM5 did not form cross-bridges. DelM2 lacking 295 amino acids from the carboxyl-terminal tail formed apparently short cross-bridges, whereas DelM3 and DelM4, having tail domains that are 100 amino acid shorter than wild-type NF-M, formed cross-bridges that were slightly shorter than those of the wild-type NF-M and Mmyc mutant. These data indicate that the carboxyl-terminal tail domain of NF-M is the actual compartment of the protein concerned in cross-bridge structures. Bars in the figure indicate the length of the cross-bridge ± SEM ($n = 100$) for each deletion mutant.

tach from the core filaments, they form cross-bridges. This is consistent with the two-step assembly model of neurofilaments, in which core filaments with no crossbridges are first formed, and as these filaments accumulate so that individual filaments are close enough to form cross-bridges, the carboxyl-terminal tail domains of NF-M project to interact with each other to form cross-bridges (Fig. 13).

## Discussion

### The Carboxyl Tail Domains of NF-M and NF-H both Form Cross-bridge Structures In Vivo

Our experiments give direct evidence for the first time that the carboxyl-terminal tail domain of NF-M does indeed form cross-bridge structures in vivo. The cross-bridges were identified between adjacent neurofilaments, as well as between neurofilaments and membranous organelles. They quite resemble those found in axons (Hirokawa, 1982; Hirokawa et al., 1984). Previous immunocytochemical and reconstitution studies indicated that the NF-H carboxyl-terminal tail domain is a component of cross-bridges between adjacent neurofilaments. Then a question would arise: what are the functional differences between NF-M and NF-H? The first point to be made is that NF-M and NF-H may be functionally distinct cross-linkers. Our previous studies showed that the carboxyl-terminal tail domain of NF-H interacts with tubulin in a phosphorylation-dependent manner (Hisanaga and Hirokawa, 1990a; Miyasaka et al., 1993). On the other hand, in NF-L- and NF-M-transfected Sf9 cells, we did not observe any cross-bridges between neurofilaments and microtubules, although this issue does require more detailed and intensive studies. Thus, it is possible to interperate that NF-M is an interneurofilament cross-linker, while NF-H has interneurofilament and microtubule cross-linking activity in addition to interneurofilament cross-linking. The possibility, however, that NF-M also interacts with microtubules in a phosphorylation-dependent manner, as is the case with NF-H, still remains. Our study of neurofilaments in the juvenile axon, which expresses NF-L and NF-M, but not NF-H, revealed cross-bridges between neurofilaments and microtubules (Hirokawa et al., 1984). This evidence suggests that NF-M could also form cross-bridges between neurofilaments and microtubules. Therefore, a definitive answer to this point awaits further studies on the phosphorylation of NF-M. Also, the existence of cross-bridges between neurofilaments and small membranous organelles, which was observed in our transfection experiments, should not be ignored as another function of NF-M (Fig. 6 *B*).



*Figure 13.* Two-step assembly model of neurofilaments. NF-Ls by themselves form short fragmented filaments with no cross-bridges. However, when NF-L and NF-M are expressed together, they form parallel filaments linked to each other with frequent cross-bridges. Monomers of NF-L and NF-M first polymerize to form longitudinally elongated 10-nm filaments with no cross-bridges. As these filaments accumulate, the carboxyl-terminal tail domain of NF-M hangs out from the filament to form cross-bridge structures. Although the structures formed by NF-L and NF-M have cross-bridges, we call them premature neurofilaments since they lack NF-H. The carboxyl-terminal tail domains of NF-Ms may either interact with each other (*B*), or they may interact directly with the core filaments (*A*) to form cross-bridges.

The second point that deserves attention is the difference in phosphorylation diversity between NF-M and NF-H. In our experiments, phosphorylation of the transfected proteins were uncontrollable. However, the Sf9-baculovirus system guarantees phosphorylation similar to those in native form to a certain extent. Indeed, NF-M expressed in Sf9 cells were recognized by an antibody that recognizes its phosphorylated form. NF-M expressed with NF-L showed strong bundling activity in Sf9 cells, and this activity might be phosphorylation dependent. Therefore, it remains to be determined whether there is any relationship between phosphorylation and neurofilament bundling activity for these proteins. By expressing NF-L and mutant rat NF-M with all six serines in the putative phosphorylation sites in the tail domain substituted to aranin in Sf9 cells, we may see the effect of phosphorylation on filament bundling or on cross-bridge formation.

The third point to be addressed is the developmental expression patterns of NF-M and MF-H. They are expressed much earlier in development than NF-H, which is only expressed after birth in mice (Shaw and Weber, 1982; Pachter and Liem, 1984; Charnas et al., 1992). Our experiments give insight into what is taking place at the stage of development when NF-H is not yet expressed. At this stage, neurofilaments already exist in axons, and they have the ability to form parallel-organized core filaments linked to each other with frequent cross-bridges such as those structurally similar to mature neurofilaments. However, the frequency of cross-bridges in these juvenile axons is not as high as that in adults. In our transfection experiments expressing only NF-L and NF-M without NF-H, the frequency of cross-bridges was slightly lower than that of mature axons. This might be caused by the lacking function of NF-H. Thus, it could be hypothesized that NF-L and NF-M build the basic structure of neurofilaments, and the additional expression of NF-H with its phosphorylation might function to augment or modify the premature neurofilaments.

## Assembly Mechanism of Neurofilaments Deduced from Deletion Mutant Analysis of NF-M

The mechanism of how neurofilaments assemble is not fully understood, although our recent photobleaching studies showed that they are dynamically turned over in the axons (Okabe et al., 1993; Takeda et al., 1994).

Our deletion mutant studies of the NF-M tail domain revealed that this domain is the actual component of cross-bridge structures. At the same time, this domain is involved in longitudinal extension and elongation of the core filaments. In contrast, NF-Ls by themselves are only able to form short fragmented filaments, and in some cases, these fragments form aggregates. Viewed by quick-freeze, deep-etch electron microscopy, filaments polymerized by either L + DelM1 or L + DelM5 resemble those of NF-L alone. On the other hand, all L + DelM2, L + DelM3, and L + DelM4 polymerize into filaments that are relatively straight and longitudinally extended. Cross-bridges are also observed in these three filaments. As a whole, the latter three form filaments that are close to those formed by the wild-type NF-L and NF-M. This suggests that amino acid sequences included in DelM2, DelM3, and DelM4 are responsible for the activity that induces longitudinal extension of the core filaments.

How the carboxyl-terminal tail domain can affect core filament assembly would be the next question. Two models can be proposed. Firstly, longitudinal extension of the core filaments is induced by the cross-bridge-forming activity of the NF-M tail domain. In this model, core filament assembly and cross-bridge formation occur at the same time, when NF-L and NF-M copolymerize. In other words, the polymerization of neurofilaments is equivalent to the formation of the highly ordered neurofilament ultrastructure. The other model is based on a two-step assembly hypothesis of neurofilaments (Fig. 13). By this concept, neurofilaments first polymerize into 10-nm filaments that have no cross-bridges and, as the filaments come into close contact, projections of the carboxyl-tail domains of NF-M occur to form cross-bridge structures that determine the spacings between the filaments. Core filament assembly with no cross-bridges occurs first, and then cross-bridges are formed. According to this model, NF-M carboxyl terminal tail domains serve the newly formed core filaments as longitudinal filament extenders before they appear to form cross-bridges. As filaments come into close proximity, the tail domains of NF-M project to interact with the filaments nearby to form cross-bridges. Whether two tail domains on different filaments directly interact to form cross-bridges is not clear. Cross-bridges may be formed by interaction of the NF-M tail domain of one filament with the core of another filament. The precise molecules or domains that interact with the NF-M tail remain to be determined.

In our experiments, transfection of DelM2, DelM3, or DelM4 with NF-L results in filaments with a small number of cross-bridges, and this is not caused by the overexpression of NF-L relative to deletion mutants, since, even though NF-L is expressed four times more in molar ratio, the L + Mmyc virus forms filaments with frequent cross-bridges. Because mild permeabilization disrupts the parallel tendency of filament organization, the low frequency of cross-bridges may be caused by the reduced interacting force generated by the cross-bridges. Thus, the longitudinal extending activity of the core filaments is not dependent on the number of cross-bridges formed. Therefore the two-step assembly model of neurofilaments is strongly supported by our data (Fig. 13), and the ultrastructural data about early developmental stages when only NF-L and NF-M are expressed (Hirokawa et al., 1984) also support this model.

## Different Segments in the Carboxyl-terminal Tail of NF-M Have Overlapping Function

The carboxyl-terminal tail domain of NF-M has repeated sequence motifs such as KSP putative phosphorylation sites. Although there are many antibodies that react with known epitopes within the tail domain, detailed functional analysis of the tail based on amino acid sequences is still far from complete. In our experiments, deletion mutants DelM2 and DelM4 contain different parts of the tail domain with four amino acids in common. Nevertheless, both mutants form long intermediate filaments with NF-L, and they contribute to some cross-bridge formation. Likewise, DelM2, DelM3, and DelM4 are all different constructs, but the phenotypes of the filaments formed with NF-L are quite similar. This means that different regions of the tail domain have similar functions, especially in the region where phosphorylation sites are scattered. In contrast, the region of 100 amino acids

from the carboxyl-terminal seems to have different properties which is suggested by comparing L + DelM2 and L + DelM5 transfections. Our experiments, therefore, suggest that the tail domain of NF-M may consist of two functionally distinct regions. One is the region that occupies 75% of the amino acids part of the tail that includes all of the putative phosphorylation sites. This region is concerned with cross-bridge formation and longitudinal filament elongation. Different parts within this region seem to be functionally homogenous and exchangeable, as shown in L + DelM2 and L + DelM4 experiments. The other region is the last 100 amino acids of the molecule. This region is not necessary for cross-bridge formation since DelM2 and DelM3, which lack this part, are capable of forming cross-bridges with NF-L. The precise function of this region awaits more detailed studies.

## Phosphorylation of the Carboxyl Terminal Tail Domain of NF-M

Six different phosphorylation sites are identified in the carboxyl-terminal tail domain of rat NF-M (Zu et al., 1993). Phosphorylation in the amino terminal head domain of NF-M is known to influence core filament assembly and disassembly (Nixon and Sihag, 1991). Studies in Trembler mice revealed that the local increase of neurofilament density is correlated, to some extent, to the hypophosphorylation of the carboxyl-terminal tail domain of both NF-M and NF-H (de Waegh et al., 1992). Little is known, however, about the precise meaning of phosphorylation in the carboxyl-terminal tail domain of NF-M. Rat NF-M is also used in our study. DelM1 and DelM5 do not include any phosphorylation sites in the carboxyl tail. DelM2 and DelM4 each bear three phosphorylation sites in the tail domain. Furthermore, DelM3 possesses all previously known tail domain phosphorylation sites. The behavior of the assembly of deletion mutant NF-Ms with NF-L fell into two types in our transfection experiments. For transfection of L + DelM1 and L + DelM5 viruses, filament assembly was complicated, random in organization, and aggregated in some cases. The filaments formed were apparently short, lacking longitudinal extension and, above all, no cross-bridges were observed. On the other hand, L + DelM2, L + DelM3, and L + DelM4 viruses formed relatively long and longitudinally extended filaments with a low frequency of cross-bridge structures. The difference in assembly patterns between the first two (L + DelM1 and L + DelM5) and the other three was obvious from the quick-freeze, deep-etch electron micrographs. The former two do not bear any phosphorylation sites in the tail domain, but the latter three do. Therefore, the existence of the putative phosphorylation sites in the tail domain of mutant NF-Ms correlates with longitudinally extended filament formation, and all these sites are included in the portion of the tail that actually constitutes cross-bridge structures. This strongly supports the concept that the cross-bridge formation and neurofilament density may be modulated by the phosphorylation of the tail domain, such as indicated in the case of Trembler mice (de Waegh et al., 1992) and other hypomyelinated transgenic mice (Cole et al., 1994). Whether phosphorylation of the NF-M carboxyl-terminal tail domain is identical to the situation in axons is unknown in transfected Sf9 cells. Strong relation between cross-bridge structures

and phosphorylation has been suggested by many studies, since NF-M has a similar molecular motif to NF-H. Finally, based on the two-step assembly mechanism of neurofilaments, we propose that phosphorylation in the carboxyl-terminal of NF-M might influence the property of core filaments when they are still not projecting from the core filament to form cross-bridges. Here, we conclude that the carboxyl-terminal tail domain of NF-M has a functional role in the longitudinal extension of the core filaments, even when they do not form cross-bridges.

## References

Charnas, L. R., B. G. Szaro, and H. Gainer. 1992. Identification and developmental expression of novel low molecular weight neuronal intermediate filament protein expressed in Xenopus laevis. J. Neurosci. 12:3010–3024.

Chen, J., Y. Kanai, N. J. Cowan, and N. Hirokawa. 1992. Projection domains of MAP2 and tau determine spacings between microtubules in dendrites and axons. Nature (Lond.). 360:674–677.

Chin, S. S. M., and R. K. H. Liem. 1989. Expression of rat neurofilament proteins NF-L and NF-M in transfected non-neuronal cells. Eur. J. Cell Biol. 50:475–490.

Chin, S. S. M., and R. K. H. Liem. 1990. Transfected rat high-molecular-weight neurofilament (MF-H) coassembles with vimentin in a predominantly nonphosphorylated form. J. Neurosci. 10:3714–3726.

Chin, S. S. M., P. Macioce, and R. K. H. Liem. 1991. Effects of truncated neurofilament proteins on the endogenous intermediate filaments in transfected fibroblasts. J. Cell Sci. 99:335–350.

Ching, G. Y., and R. K. H. Liem. 1993. Assembly of type IV neuronal intermediate filaments in nonneuronal cells in the absence of preexisting cytoplasmic intermediate filaments. J. Cell Biol. 122:1323–1335.

Cole, J. S., A. Messing, J. Q. Trojnowski, and V. M. Y. Lee. 1994. Modulation of axon diameter and neurofilaments by hypomyelinating Schwann cells in transgenic mice. J. Neurosci. 14:6959–6966.

Cote, F., J. F. Collard, and J. P. Julian. 1993. Progressive neuropathy in transgenic mice expressing the human neurofilament heavy gene: a mouse model of amyotropic lateral sclerosis. Cell. 73:35–46.

de Waegh, S. M., V. M. Y. Lee and S. T. Brady. 1992. Local modulation of neurofilament phosphorylation, axonal caliber, and slow axonal transport by myelinating Schwann cells. Cell. 68:451–463.

Eyer, J., and A. Peterson. 1994. Neurofilament-deficient axons and perikaryal aggregates in viable transgenic mice expressing a neurofilament-beta-galactosidase fusion protein. Neuron. 12:389–405.

Friede, R. L., and T. Samorajski. 1970. Axon caliber related to neurofilaments and microtubules in sciatic nerve fibers of rats and mice. Anat. Rec. 167:379–388.

Harris, J., C. Ayyub, and G. Shaw. 1991. A Molecular dissection of the carboxy terminal tails of the major neurofilament subunits NF-M and NF-H. J. Neurosci. Res. 30:47–62.

Hirokawa, N., and J. E. Heuser. 1981. Quick-freeze, deep-etch visualization of the cytoskeleton beneath surface differentiations of intestinal epithelial cells. J. Cell Biol. 91:399–409.

Hirokawa, N. 1982. Cross-linker system between neurofilaments, microtubules, and membranous organelles in frog axons revealed by the quick-freeze, deep-etch method. J. Cell Biol. 94:129–142.

Hirokawa, N., M. A. Glicksman, and M. B. Willard. 1984. Organization of mammalian neurofilament polypeptides within the neuronal cytoskeleton. J. Cell Biol. 98:1523–1536.

Hirokawa, N. 1986. 270K microtubule-associated protein cross-reacting with anti-MAP2 IgG in the crayfish peripheral nerve axon. J. Cell Biol. 103:33–39.

Hirokawa, N., and H. Yorifuji. 1986. Cytoskeletal architecture in the reactivated crayfish axons with special reference to the crossbridges between

microtubules and membrane organelles and among microtubules. *Cell. Motil. Cytoskeleton.* 6:458–468.

Hisanaga, S., and N. Hirokawa. 1988. Structure of the peripheral domains of neurofilaments revealed by low angle rotary shadowing. *J. Mol. Biol.* 202:297–305.

Hisanaga, S., and N. Hirokawa. 1990a. Dephosphorylation-induced interactions of neurofilaments with microtubules. *J. Biol. Chem.* 265:21852–21858.

Hisanaga, S., and N. Hirokawa. 1990b. Molecular architecture of the neurofilament 2. Reassembly process of neurofilament L protein in vivo. *J. Mol. Biol.* 211:871–882.

Hoffman, P. N., J. W. Griffin, and D. L. Price. 1984. Control of axonal caliber by neurofilament transport. *J. Cell Biol.* 99:705–714.

Hoffman, P. N., G. Thompson, J. Griffin, and D. Price. 1985. Changes in neurofilament transport coincide temporally with alterations in the caliber of axons in regenerating motor fibers. *J. Cell Biol.* 101:1332–1340.

Hoffman, P. N., D. W. Cleveland, J. W. Griffin, P. W. Landes, N. J. Cowan, and D. L. Price. 1987. Neurofilament gene expression: A major determinant of axonal caliber. *Proc. Natl. Acad. Sci. USA.* 84:3472–3476.

Lasek, R. J., M. Oblinger, and P. Drake. 1983. Molecular biology of neuronal geometry: expression of neurofilament genes influences axonal diameter. *Cold Spring Harbor Symp. Quant. Biol.* 18:731–744.

Lee, V. M. Y., L. Otvos, Jr., M. J. Carden, M. Hollosi, B. Dietzschold, and R. A. Lazzarini. 1988. Identification of the major multiphosphorylation site in mammalian neurofilaments. *Proc. Natl. Acad. Sci. USA.* 85:1998–2002.

Lee, M. K., Z. Xu, P. C. Wong, and D. W. Cleveland. 1993. Neurofilaments are obligate heteropolymers in vivo. *J. Cell Biol.* 122:1337–1350.

Lee, M. K., and D. W. Cleveland. 1994. Neurofilament function and dysfunction: involvement in axonal growth and neuronal disease. *Curr. Opin. Cell Biol.* 6:34–40.

Levy, E., R. K. H. Liem, P. D'Eustachio, and J. N. Cowan. 1987. Structure and revolutionary origin of the gene encoding mouse NF-M, the middle-molecular-mass neurofilament protein. *Eur. J. Biochem.* 166:71–77.

Miyasaka, H., S. Okabe, K. Ishigro, T. Uchida, and N. Hirokawa. 1993. Interaction of the tail domain of high molecular weight subunits of neurofilaments with the COOH-terminal region of tubulin and its regulation by tau kinase II. *J. Biol. Chem.* 26:22695–22702.

Monterio, M. J., and D. W. Cleveland. 1989. Expression of NF-L and NF-M in fibroblasts reveals coassembly of neurofilament and vimentin subunits. *J. Cell Biol.* 108:579–593.

Napolitano, E. W., S. S. M. Chin, D. R. Colman, and R. K. H. Liem. 1987. Complete amino acid sequence and in vitro expression of rat NF-M, the middle molecular weight neurofilament protein. *J. Neurosci.* 7:2590–2599.

Nixon, R. A., and R. K. Sihag. 1991. Neurofilament phosphorylation: a new look at regulation and function. *Trends Neurosci.* 14:501–506.

O'Reilly, D. R., L. K. Miller, and V. A. Luckow. 1992. Baculovirus Expression Vectors. A Laboratory Manual. W. H. Freeman and Company, Oxford, England. 347pp.

Okabe, S., H. Miyasaka, and N. Hirokawa. 1987. Dynamics of neuronal intermediate filaments. *J. Cell Biol.* 121:375–386.

Okayama, H., M. Kawaichi, M. Brownstein, F. Lee, T. Yokota, and K. Arai. 1987. High-efficiency cloning of full-length cDNA: construction and screening of cDNA expression libraries for mammaliam cells. *Methods Enzymol.* 154:3–28.

Osborn, M., and K. Weber. 1987. Cytoplasmic intermediate filament proteins and the nuclear lamins A, B and C share the IFA epitope. *Exp. Cell Res.* 170:195–203.

Pachter, J. S., and R. K. H. Liem. 1984. The differential appearance of neurofilament triplet polypeptides in the developing rat optical nerve. *Dev. Biol.* 103:200–210.

Pruss, R. M., R. Mirsky, M. C. Raff, R. Thorpe, A. J. Dowding, and B. H. Anderton. 1981. All classes of intermediate filaments share a common antigenic determinant defined by a monoclonal antibody. *Cell.* 27:419–428.

Riemer, D., H. Dodemont, and K. Weber. 1991. Cloning of the non-neuronal intermediate filament protein of the gastropod *Aplysia carfornica*; identification of an amino acid residue essential for the IFA epitope. *Eur. J. Cell Biol.* 56:351–357.

Sambrook, J., E. F. Fritsch, and T. Maniatis. 1989. Molecular Cloning: A Laboratory Manual. Cold Spring Harbor Laboratory Press, Cold Spring Harbor, NY.

Shaw, G., and K. Weber. 1982. Differential expression of neurofilament triplet proteins in brain development. *Nature (Lond.).* 298:277–279.

Sternberger, L. A., and N. H. Sternberger. 1983. Monoclonal antibodies distinguish phosphorylated and nonphosphorylated forms of neurofilament in situ. *Proc. Natl. Acad. Sci. USA.* 80:6126–6130.

Takeda, S., S. Okabe, T. Funakoshi, N. Hirokawa. 1994. Differential dynamics of neurofilament H protein and neurofilament L protein in neuron. *J. Cell Biol.* 127:173–185.

Viancour, T. A., K. R. Seshan, G. D. Bittner, and R. A. Sheller. 1987. Organization of axoplasm in crayfish giant axons. *J. Neurocytol.* 16:557–566.

Volkman, L. E., and K. J. M. Zaal. 1990. *Autographa californica* M nuclear polyhedrosis virus: microtubules and replication. *Virology.* 175:293–302.

Wong, P. C., and D. W. Cleveland. 1990. Characterization of dominant and recessive assembly-defective mutations in mouse neurofilament NF-M. *J. Cell Biol.* 111:1987–2003.

Willard, M., and C. Simon. 1981. Antibody decoration of neurofilaments. *J. Cell Biol.* 89:198–205.

Zu, Z. S., W. S. Liu, and M. B. Willard. 1992. Identification of six phosphorylation sites in the COOH-terminal tail region of the rat neurofilament protein M. *J. Biol. Chem.* 267:4467–4471.

Zu, Z., L. Cork, J. Griffin, and D. W. Cleveland. 1993. Increased expression of neurofilament NF-L produces morphological alterations that resemble the pathology of the human motor disease. *Cell.* 73:23–33.